Level Measurement using ultrasound

Håkon Bøe

Problem description

Selective Catalytic Reduction (SCR) [2] is a system in place to reduce NOx emissions from diesel engines. SCR does this by reducing NOx into nitrogen and water. In this process, a liquid known as Diesel Exhaust Fluid (DEF), popularly called Adblue, is used as a reducing agent. The Adblue is sprayed into the exhaust stream where a catalyst combines the exhaust with the Adblue to achieve reducing of the NOx. The Adblue is stored in a separate tank in the vehicle, where an accurate level measurement is necessary because of a need for consumption monitoring. Additionally, the system can be damaged if other liquids than Adblue is filled into the DEF tank. This thesis will explore the possibilities of estimating the level in such a tank, using an ultrasonic sensor. The thesis is an extension of report written by the author where the level was estimated without the presence of noise. This work can be found in [5]. The goal of the thesis will be to:

1. Conduct experiments with the presence of noise in the form of bubbles, disturbances in the liquid surface and tilting

2. Extend the algorithm developed for echo detection presented in [5] as to cope with the presence of noise in the form of vibration and temperature changes.

3. Explore how to detect the presence of a diesel layer on top of the diesel exhaust fluid (DEF).

Preface

This master thesis concludes my degree from the Department of engineering cybernetics at the Norwegian University of Science and Technology. This thesis has been conducted both with and for Wema System AS. I would like to thank Wema personnel for assisting me with my thesis. I would also like to thank my fellow students at room G238 for lending me your advice: Håkon Søhoel, Øyvind Halvorsen, Erlend Kvinge Jørgensen, Kristian Stormo, Simen Fuglaas. I would also like to thank my supervisor Tor Onshus.

iv

Abstract

This thesis describes the development and performance of a level measurement system based on estimating the round-trip-time of an ultrasonic signal. A new prototype is designed and constructed, built on the foundations of an ultrasonic speed of sound measurement system made by Wema System AS. Tests are performed and data is recorded under noisy conditions, such as vibrations created by a vibration bench at Wema HQ, and also simulated temperature changes, such as the presence of bubbles in the liquid.

Different procedures for trigging the transducer is compared in terms of noise resistance and signal strength.

Software is developed in Matlab as to detect ultrasonic echoes and estimate the Round-trip-time for the ultrasonic signal as to calculate a level-estimate. Properties related to the success of said software are explored, such as signal strength as a function of liquid level. A software model in k-wave is developed to simulate the ultrasonic signal propagating in an environment similar to that of the system.

Finally, tests are conducted with the presence of a diesel layer on top of the DEF. A procedure for detecting a diesel layer on top is suggested, based on experimental data.

Samandrag

Denne oppgåva beskriv utvikla og ytelsen av eit nivå-målingsystem basert
på å estimere tur- og returtida til eit ultralydsignal. Ein ny prototype
vert utvikla og bygd, basert på eit måleoppsett for lydhastighetsmålingar
med ultralyd utvikla av Wema System As. Måledata vert tatt opp under
støyfulle forhold i form av vibrasjonar, og simulerte temperaturendringar
ved å tilsette bobblar i målevæska.

Ulike metodar for å påtrykke transduseren spenningsdifferansar vert
samanlikna med tanke på signalstyrke og ytelse under støyfulle forhold.

Mjukvare vert utvikla i Matlab for å detektere ultralydekko og kalkulere
tur- og returtida for å kunne estimere væskenivået. Egenskapar knytta til
signalet vert utforska, som signalstyrken som ein funsksjon av væskenivået
i prototypen. Ein simuleringsmodell vert utvikla i ein ultralydssimulator
kalla k-wave, for å simulere utralydssignalet.

Moglegheita for å detektere eit diesellag på toppen av eit lag med DEF
vert foreslått, basert på eksperimentell data.

Conclusion

The robustness of the system when subjected to noise is crucially dependent on signal strength. The signal strength is proven to be varying with the liquid level in the prototype, and a simulation framework is developed. The simulation tool can be used as a guideline for finding the pipe radius which has the best overall signal strength for the entire range in liquid level for the system. The 580 kHz trigger performs best in terms of signal strength both in the vibrations tests and the temperature tests. By changing the filter coefficients in the bandpass filter, the 580 kHz trigger's magnitude can be increased further. The performance of the algorithms presented in this thesis is tested and the results are presented. The error in accuracy of the calculated round-trip-time (RTT) in the vibration tests are quite significant - up to 1 cm difference in level at maximum. By manual inspection it is seen that the algorithms perform as expected. A likely cause for this is believed to be that the prototype pipe is not fastened enough as to not shift position during the vibration tests, causing an offset of the pre-level calculation. The presence of diesel layers can be detected for the experimental data presented in this thesis. However it is noted that the difficulty of detecting this will depend on the thickness of the different layers. Indications of a diesel layer in the ultrasonic signal include:

x

- The echo with the largest amplitude is not the first echo in the measurement.

- Multiple echoes which have round-trip-times which are not a multiple of each other are detected

- The power spectrum density is significantly different between the first and the main echo.

Contents

List of Figures

Chapter 1

Introduction

The emission of NO_x gasses in the road transport sector have been reduced by 48 % in the period 1990-2011. Still, in 2011, the road transport sector is behind 41 % of the total NO_x emission [1]. A system that can be used to reduce the NOx emissions from diesel engines are the Selectie Catalytic Reduction (SCR) [2]. The SCR is dependent on an urea solution called adblue. The adblue is stored in a separate tank in the vehicle. In order for the vehicle operator to know the amount of adblue left in the tank, the amount of liquid in the tank needs to be monitored. A technique that can be used for such measurements is based on the propagation of ultrasonic waves. This is a technique that was developed almost 50 years ago [3]- [4].

This report explores a level measurement system using an ultrasonic transducer to estimate the amount of liquid left in such a tank. This work is a continuation to the work done in [5], with the inclusion of noise in the form of temperature changes in the tank, and vibration. The possibilities of detecting the presence of a diesel layer on top of the adblue is also explored.

A new prototype is made and used in a vibration bench to test the effects

of vibrations on the measurement system and the software algorithms for calculating the round-trip-time of the ultrasonic signal. Different methods for trigging the piezo-electric element in the transducer are compared in terms of signal strength under noisy conditions. To simulate temperature changes, bubbles are added in the liquid to test the effect on the ultrasonic signal. Experiments and simulations are compared in order to understand how the amplitude of the surface echo changes at different levels.

Chapter 2

Theory

2.1 System overview

The system is portrayed in figure 2.1.

Floater

Tank

Pipe

Holes

Transducer

Trigger

To signal processing
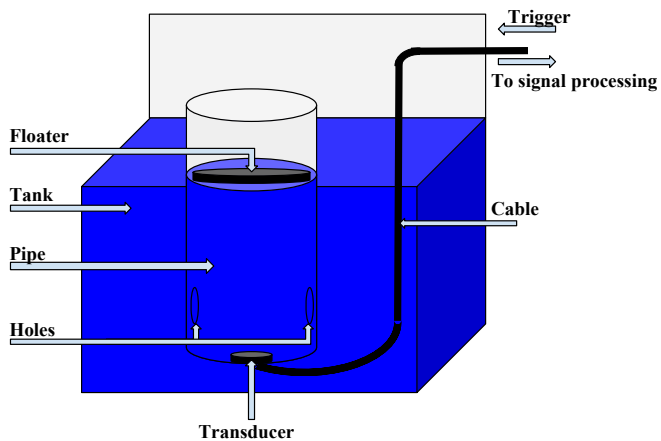
Cable

Figure 2.1: System Overview

The transducer is mounted at the bottom of a plastic pipe. Connected to the transducer is a cable that carries both the trigger and the received signal. The trigger is a voltage signal that is used to make the piezo-element expand and contract in its resonance frequencies. This creates an ultrasonic wave which travels along the pipe until it hits floater. The floater has a reflective steel plate attached to it which is pointing against the transducer, as to reflect the incoming ultrasonic wave back to the transducer. The plastic pipe has two holes cut into it, as to let liquid flow between the tank and the pipe. Thus, by measuring the time-of-flight of an ultrasonic wave, the level can be calculated using the following formulae:

$$d = \frac{1}{2} \triangle t \cdot c \tag{2.1}$$

where d is the level in the pipe, $\triangle t$ is the time of flight, and c is the soundspeed in the medium.

The signal processing part is in figure 2.1 is depicted in figure 2.2
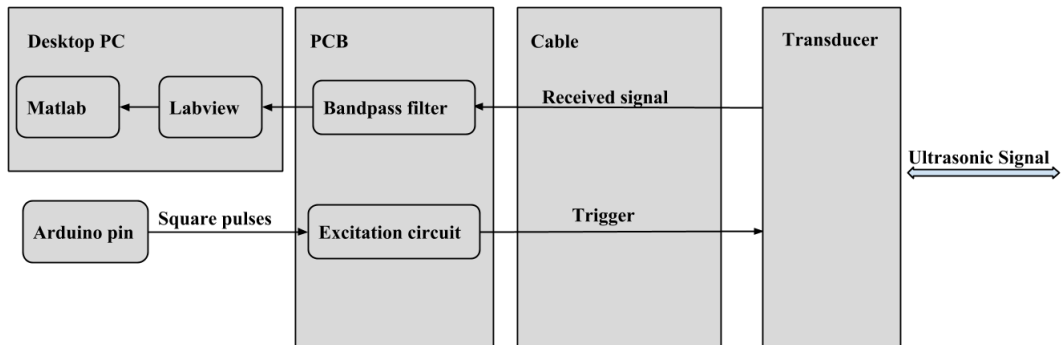
Figure 2.2: Measurement system overview

An Arduino board is used to create a series of square pulses of voltage which is applied to the excitation circuit. The excitation circuit is located on the Programmable Circuit Board (PCB) made by Wema. A signal cable then carries the trigger to the transducer which will create an ultrasonic signal. The received signal is then recorded by a Labview application after being filtered through an analogue bandpass filter. The data is logged into files of raw data which can be processed in Matlab offline.

The transducer, cable and PCB is supplied and made by Wema. Modifications such as connection the arduino pin to the PCB and measuring the voltage at the exit of the bandpass filter is constructed by the author.

An illustration of the resulting recorded ultrasonic signal can be seen in figure 2.3. This figure is found in [5].
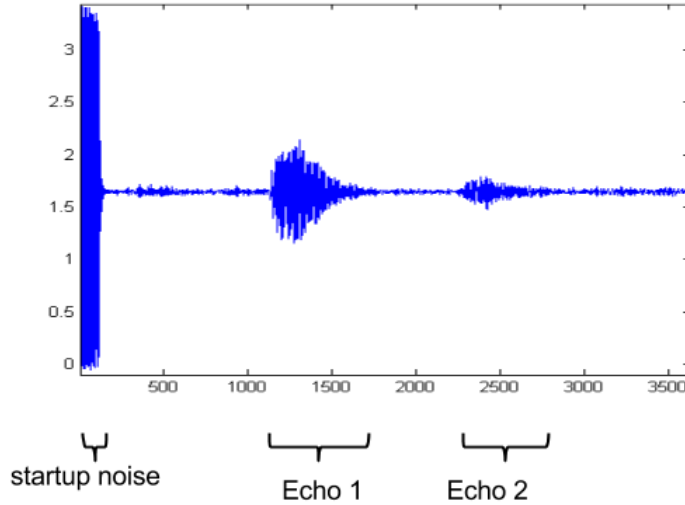
Figure 2.3: Ultrasonic signal recorded in adblue

2.2   The wave equation

An acoustic wave propagating in a medium can be described by the inhomogeneous wave equation:

$$\nabla^2 p - \frac{1}{c_0}\frac{\partial^2 p}{\partial t^2} = \rho_0 \frac{\partial f(r,t)}{\partial t} \tag{2.2}$$

where p is the sound pressure, c_0 is the sound speed in the medium, ρ_0 is the density in the medium, and $f(r,t)$ is the source term.

Another variable that can describe a sound wave is the particle veloc-
ity. Particle velocity is the speed which a particle fluctuates with around
its equilibrium when an acoustic wave passes through a medium. Particle
velocity is a 3D-vector, but it is sometimes more convenient to describe the
wave with a scalar. The velocity potential is defined as

$$\boldsymbol{v} = \nabla \phi \tag{2.3}$$

The relation between sound pressure and velocity potential is given as

$$p = -\rho_0 \frac{\partial \phi}{\partial t} \tag{2.4}$$

The velocity potential can then be written similarly to equation 2.2,

$$\nabla^2 \phi - \frac{1}{c_0} \frac{\partial^2 \phi}{\partial t^2} = -f(r, t) \tag{2.5}$$

The Laplacian operator ∇ is dependent on the coordinate system used.
As the ultrasonic wave is to propagate in a cylinder, a cylindrical coordinate
system is convenient for this system. In cylindrical coordinates, the Laplace
operator is written as

$$\nabla^2 \phi = \frac{1}{r} \frac{\partial}{\partial t} (r \frac{\partial \phi}{\partial r}) + \frac{1}{r^2} \frac{\partial^2 \phi}{\partial \theta^2} + \frac{\partial^2 \phi}{\partial z^2} \tag{2.6}$$

where θ is the azimuth angle.

Unfortunately, a trivial form of the solution to the cylindrical wave equa-
tion in the time domain does not exist.

2.3   Solving the wave equation

In chapter 2.2 equation 2.5 describes the velocity potential in the time domain. It was noted that this equation does not have a trivial solution in cylindrical coordinates. However, by applying the Fourier transform

$$\Phi(\omega) = \int_{-\infty}^{\infty} \phi(t))e^{i\omega t}dt \tag{2.7}$$

on equation 2.5, the inhomogeneous Helmholtz equation can be written as

$$[\bigtriangledown^2 + \kappa^2]\Phi(\boldsymbol{r},\omega) = -F(\boldsymbol{r},\omega) \tag{2.8}$$

where $F(\boldsymbol{r},\omega)$ is the Fourier transform of the source term in equation 2.5, $\boldsymbol{r}$ is the coordinates, and κ is the wave number defined as

$$\kappa = \frac{\omega}{c_0} \tag{2.9}$$

The Helmholtz equation solved for a 2D circular piston transducer is given as

$$\Phi(r,\theta) = \frac{Q}{4\pi r}\frac{2J_1(\kappa a sin\theta)}{\kappa a sin\theta}e^{i\kappa r} \tag{2.10}$$

Where Q is the source strength, and J_1 is the Bessel function of first order, first kind. Note that this solution is only valid in the far-field, that is, the distance from the transducer is greater than the Rayleigh distance given in equation 2.13.

The second fraction of equation 2.10 is called the directivity function, and is written as

$$B(\theta) = \frac{2J_1(\kappa a sin\theta)}{\kappa a sin\theta} \tag{2.11}$$

Equation 2.11 is plotted in figure 2.4.
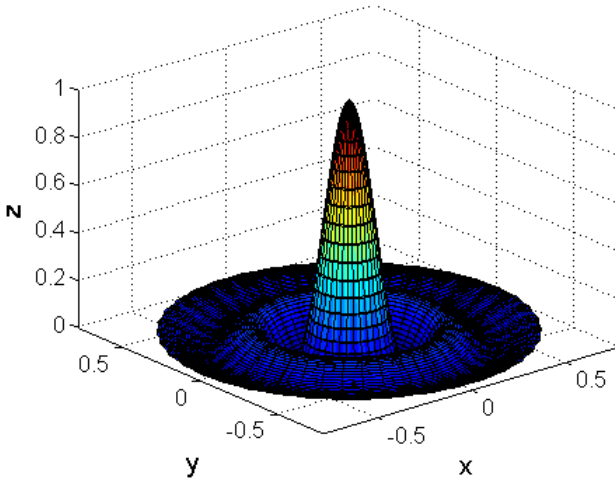
Figure 2.4: Directivity function for a circular piston transducer

2.4 Transducer properties

The transducer is circular with a radius of 0.5 cm and two resonance frequencies, one at 580 kHz and one at 1 MHz. The power spectrum density of the transducers is shown in figure 2.5.

Note that this is after being filtered by the bandpass filter as described in 2.7.
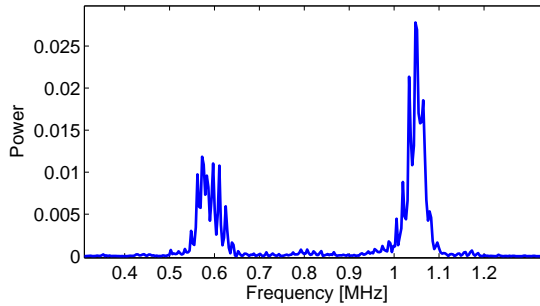
Figure 2.5: Power spectrum density

The width of the main lobe is given as

$$\Delta\theta \approx \frac{\lambda\pi}{\pi a} \qquad (2.12)$$

For the resonance frequency at 1 MHz, assuming propagation through ad-blue at room temperature, λ is given as $c/f = \frac{1630\frac{m}{s}}{1MHz} = 0.0016m$, and the width of the main lobe is given by equation 2.12 as $\Delta\theta \approx {}^{\circ}11.9$. By looking at the resonance frequency at 580 kHz, $\lambda = 0.0028m$, and the result from equation 2.12 is $\Delta\theta \approx {}^{\circ}20.5$.

Some assumptions has to be made for equation 2.12 to be valid. The most important assumption is related to the nearfield/farfield transition of the acoustic wave. Generally, the distance where the transition from nearfield to farfield occurs is at a distance

$$R_R = \pi a^2/\lambda \qquad (2.13)$$

from the transducer. The distance R_R is called the Rayleigh distance. Inserting into equation 2.13, the Rayleigh distance is found to be $R_R = 4.8cm$. Thus, at a distance larger than $4.8cm$ one may assume that the

far-field approximations hold.

2.5 Attenuation

Attenuation in the system can be approximated to be caused by two factors. Geometrical spreading and absorption in the media. Under ideal conditions in the system, i.e. constant temperature and no vibrations, it is possible to make simple estimations about the attenuation in a adblue.

The transmission loss due to geometrical spreading can be approximated in several ways. Cylindrical spreading, spherical spreading and a spreading weighted by the aperture function as given by figure 2.6.

Adblue consists of a certain percentage of urea and water. The optimal mixture in respect of the freezing point of adblue is 32.5 % urea and 67.5 % water. Due to the high water percentage in adblue, it is possible that the attenuation in adblue will be comparable to the attenuation in water. The contribution in transmission loss from attenuation for a wave with amplitude A_0 given as

$$A(r) = A_0 e^{-\alpha r} \tag{2.14}$$

α is the absorption coefficient and is given in $1/m$ and r is the distance in m from the source.

2.6 Acoustic waves and bubbles

When a gas bubble in a liquid is exposed to an acoustic wave propagating in the liquid, the bubble may scatter part of the incidence wave, thereby

leading to reduced amplitude of the wave. A gas bubble in an acoustic medium is considered a powerful scatterer.

According to [6], a bubble surrounded by liquid has a resonance frequency given by

$$f_{res} = \frac{1}{2\pi r}\sqrt{\frac{3\kappa p_0}{\rho}} \qquad (2.15)$$

where f_{res} is the natural resonance frequency of the bubble, p_0 is the ambient pressure, ρ is the density of the liquid surrounding the bubble, and κ is the polytrophic coefficient of the gas forming the bubble.

Thus bubbles with different radii will have different resonance frequencies.

As is seen in equation 2.11, the resonance frequency of the bubble is dependent on the radius of the bubble.

2.7   Bandpass filter

The piezoelectric-element used in the transducer has two resonance frequencies: one in the 1 MHz area and one in the 580 kHz area. By inspecting the electrical circuit the transfer function of the filter is found to be

$$H(s) = H_1 H_2 \qquad (2.16)$$

where both $H1$ and $H2$ are given by equation 2.17

$$H_i = \frac{\frac{-1}{R_{i1}C_{i1}}s}{s + (\frac{1}{R_{i2}}(\frac{1}{C_{i1}} + \frac{1}{C_{i2}}))s + \frac{1}{R_{i1}R_{i2}C_{i1}C_{i2}}}, i = 1, 2 \qquad (2.17)$$

As visualised in the bode plot of the transfer function in equation 2.16,
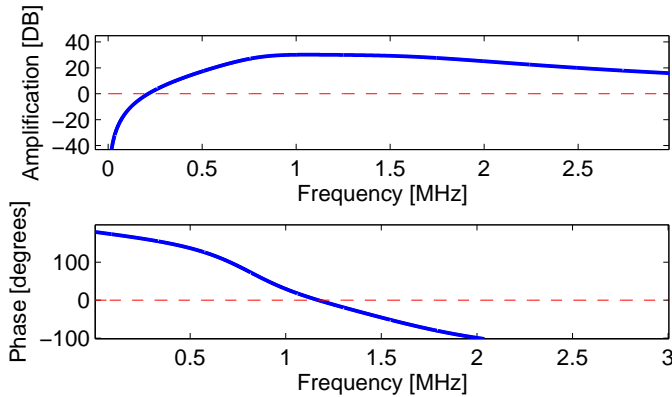
Figure 2.6: Theoretical bode plot for H

the resonance frequency of 580 kHz is not amplified as much as the one at 1 MHz. As the 580 RF is already of less power then the 1 MHz RF, it is desired to modify the filter as to amplify the 580 RF more than it is amplified as of now.

Figure 2.6 shows that the 580 kHz is not amplified with the same magnitude as the 1 MHz. There is also a certain phase shift for the 580 kHz frequency.

The values of the resistors and capacitors had to be modified to expand the bandpass of the filter as to amplify the 580 kHz RF more than it is today.

2.8   Prototype properties

2.8.1   Flow in and out of pipe

The pipe in the prototype has a flow out into the tank when the tank level is decreasing, and liquid flows into the pipe when the liquid is added into the tank. Bernoulli's equation can be used to describe the rate of flow between what can be simplifyed into a two tank system

$$\frac{v_1^2}{2} + gz_1 + p_1/\rho = \frac{v_2^2}{2} + gz_2 + p_2/\rho \tag{2.18}$$

This describes the flow between two points on the streamline in the pipe when flow is occuring from the pipe. If we choose point 1 to be the liquid surface in the pipe and point 2 to be the hole into the tank, we can make the following assumptions

1. $v_1 = 0$

2. $p_1 = p_{tank}$

3. $z_1 - z_2 = h$

where p_{tank} is the pressure inside the non-liquid containing part of the tank.

Equation 2.16 can than be rearranged to

$$v_2 = \sqrt{\frac{2}{\rho}(p_{tank} - p_2) + 2gh} \tag{2.19}$$

and the mass flow out of the pipe is then given as

$$Q = Av_2 \tag{2.20}$$

2.9   Floater buoyancy

A body at rest in a fluid has the following net force that acts upon it

$$\sum F = F_{buoyancy} - F_g = 0 \qquad (2.21)$$

from equation 2.21 it follows that

$$\rho_f V_d g = mg \qquad (2.22)$$

where ρ_f is the density of the fluid, V_d is the displaced volume by the floater, m is the mass of the floater and g is the gravitational vector.

The two fluids that will be studied in this thesis are adblue and diesel, where $\rho_{adblue} = 1087 kg/m^3$ and $\rho_{diesel} = 832 kg/m^3$. Since $\rho_{adblue} > \rho_{diesel}$ it follows from equation 2.22 that a floater that floats in adblue might not float in diesel as ρ_f decreases. If V_d cannot increase sufficiently to satisfy equation 2.22, the situation becomes $\rho_f V_d g < mg$, and the floater will sink.

2.10   Acoustic Reflection

When an acoustic wave passes through a medium and into another, the wave might be reflected back or transmitted into the new medium, or a combination of the two. The

$$R = \frac{Z_2 - Z_1}{Z_2 + Z_1} \qquad (2.23)$$

Where Z_m is the characteristic acoustic impedance given as

$$Z_m = \rho_m c_m, \ m = 1, 2 \qquad (2.24)$$

The reflection coefficient states how much of the incoming wave that is reflected back into the medium where the wave is originating from. A negative sign in the coefficient R indicates a phase shift of π radians.

2.11   Variance

Variance for a vector can be written as

$$Var(x) = \frac{1}{n} \sum_{1}^{n} (x - \mu)^2 \tag{2.25}$$

Thus for a signal ultrasonic wave normalized around zero, the mean of the signal will be ≈ 0. As the variance describes the average deviation from the mean of the signal, it suited as a measure of signal strength.

Chapter 3

Method

3.1 Measurement setup

The measurements were done similar to the setup in [5]. However, the measurement setup underwent some changes;

1. Trigger source changed

2. Increased robustness of the measurement setup

3. Labview application changes

3.1.1 Choosing a trigger source

The transducer is now triggered by an Arduino Due circuit board. The board was initially acquired because National Instruments has developed a software library that enables real time communication between an Arduino board and a Labview application running on a computer [7]. As this would make real time communication between pins on the Arduino board and the

Labview application possible, it was decided to switch to this board. The reason behind the desire for this communication is that the National Instruments board used in the measurement setup is able to take two inputs (and also a trigger for these two channels). However, if the Arduino board could communicate in real time with the measurement application, an Arduino pin could be used as input, the ADC would sample it to a digital value and send it via the Labview/Arduino interface to the computer running the application. This would for instance make it possible to measure more voltages from the PCB, as the Due card has 12 analog input pins. A property that is especially interesting is the temperature measurement accessible on the PCB, as this would make it possible to measure both the ultrasonic signal and the temperature concurrently, and log these on the computer. As the speed of sound will change with temperature, having access to the temperature measurement on the PCB would make it possible to compensate for the temperature change.

In addition, Arduino provides a software framework that is considered more easy to use than programming the micro controller in low level languages such as C. The simplified functions provided by the framework can speed up developing and is therefore a benefit from changing to an Arduino from a conventional micro controller interface.

3.1.2   Writing the trigger program

As previously stated, the Arduino Due comes with a framework that simplifies the implementation of the trigger program. Unfortunately, it was discovered that the function provided by the framework for setting a pin high was not fast enough to produce consecutive pulses of 1MHz. The function is $digitalWrite(pin, value)$, where pin is the output pin on the board

and *value* is either HIGH or LOW. Because of the inadequate functionality of this function for the trigging program, a faster way of setting the output pin high and low had to be found and tested.

The fastest way to set an output pin high and low was found to be

```
// Pin 13 mask
uint x = 27;
uint32 trig = (1u << x);

void setup(){
  REG_PIOB_OER = trig;
}

void loop() {
        REG_PIOB_SODR = trig;
        REG_PIOB_CODR = trig;
}
```

The Due has 14 digital output/input pins which can be used from trigging. By setting x, the pin can be defined. Setting x = 27 will correspond to output pin 13, which is the one used by the trigging program. The lines REG_PIOB_SODR corresponds to setting the register corresponding to the pin given by trig high, and REG_PIOB_CODR is the opposite, i.e. setting the register low [8]. Note that this is the fastest pulse the Due can create, and is discovered to be in the 2 MHz area. To be able to slow down the trigging frequency to 1MHz, the operations need to be repeated a number of times until the desired frequency is acquired.

3.1.3   Increasing the robustness of the measurement setup

As the setup was to be used to test the results from a vibrating system, the entire setup would experience more moving parts than in other tests. As the current setup at the time already experienced broken connections and loose wires when the system was to be moved, it was clear that a more robust approach was needed. The new setup for the electronics involved in the measurement setup is seen in figure 3.1
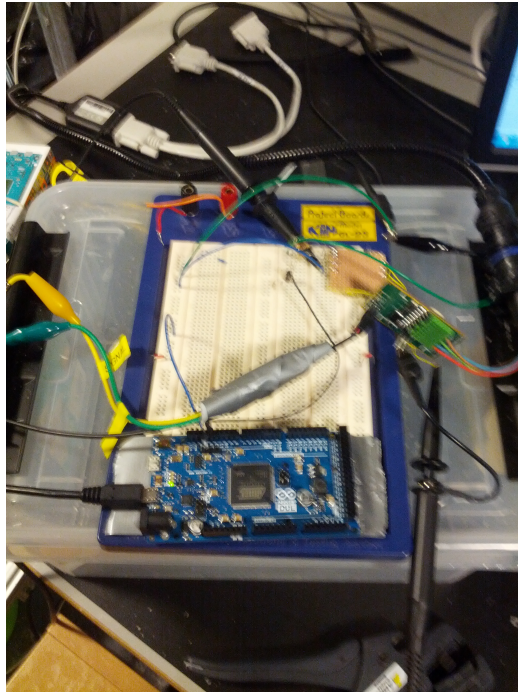
Figure 3.1: New setup electronics

3.1.4 Changing the Labview application

A problem that was discovered in [5], was that the Labview application provided by Wema did not write continuously to file when measuring. Instead the application stored all the consecutive measurements in memory, and wrote to file after the application was ended. This could lead to the program crashing when time-consuming tests were performed, and no results were available as they were cleared from memory when the application crashed. Thus it was clear that for the tests at the vibration bench, which was estimated to lasts for at least 3 hours, the application would need to log in real time.

3.2 Prototype properties

There are two main properties that are important hardware features of the prototype pipe. First, a floater is placed in the pipe, producing and offset from the actual level. While the offset is constant for all levels, it is vital to know how much of an offset this produces. Secondly, the connection between the pipe and the surrounding tank is two holes in the pipe. These holes allow liquid to travel between the tank and the pipe. Thus, it is of interest to see how the liquid level in the pipe behaves as the tank is drained.

3.2.1 Floater offset

In [5] it was determined that the system was vulnerable to slushing in the liquid surface if a floater was not used. Therefore, it was decided that a floater should be used in further investigation of the system behaviour when exposed to noise. The floater has a steel plate attached to it as to reflect the ultrasound signal to the transducer with a high reflection coefficient.
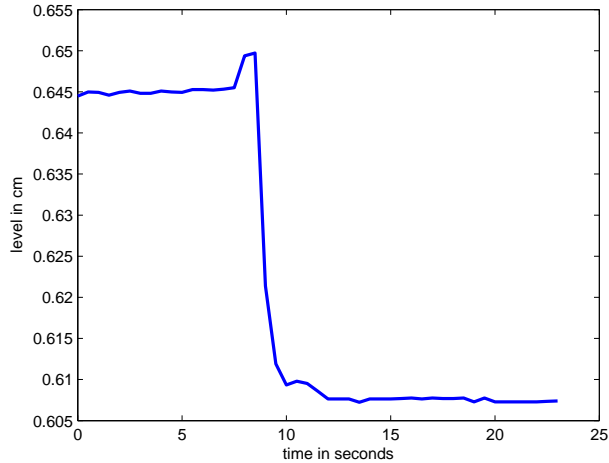
Figure 3.2: Effect of adding a floater

However, the floater produces an offset to the liquid level, as parts of the floater is emerged in the liquid.

In order to test how big the offset is, a test were performed where the liquid level is first used as the reflecting surface, and the floater is dropped into the pipe. After the offset is stabilised, the difference is then calculated.

The floater offset can be seen from figure 3.2. This is a property of the system which is important to be aware of.

3.2.2   System inertia

As in many different measurement systems, the measurements are prone to random noise. This can be effectively reduced by averaging a certain number of measurements which are consecutively in time. However, in order to average measurements, it is important that the main echo of the averaged

measurements are more or less in the same position, or else averaging will corrupt measurements instead of removing noise. The more measurements that can be averaged to form a single measurement, the more elimination of random noise. This raises the following questions regarding how the measurements are performed:

1. How often can a new measurement be perfomed

2. How fast changing is the process

The first question is dependent on how often it is possible to trig the transducer to start the vibration of the piezoelectric element and the recording of the returning vibrations. This again is dependent on the time it takes an acoustic wave to propagate to the surface of the liquid, and back. This again is dependent on the distance from the transducer to the surface, and the speed of sound in the liquid. It is vital that the main echo from the surface is received before a new measurement is started. In addition, multiple echoes might appear, and it is not desirable that echoes from a previous measurement appears during a new measurement.

The second question is more delicate. Adblue consumption during operational use depends on the vehicle, but according to [9], trucks between 7.5 - 18.5 tons use 4-10 litres of adblue a week. The reduction in level corresponding to this depends on the shape of the tank, but it is clear that this is not a fast moving process. In addition, when adblue is filled on the tank, the level will be changing more rapidly.

Data was created to simulate a rapid drainage of adblue from the tank. 1 litre of adblue was drained from the prototype. The time between trigging of the transducer was 500 ms.
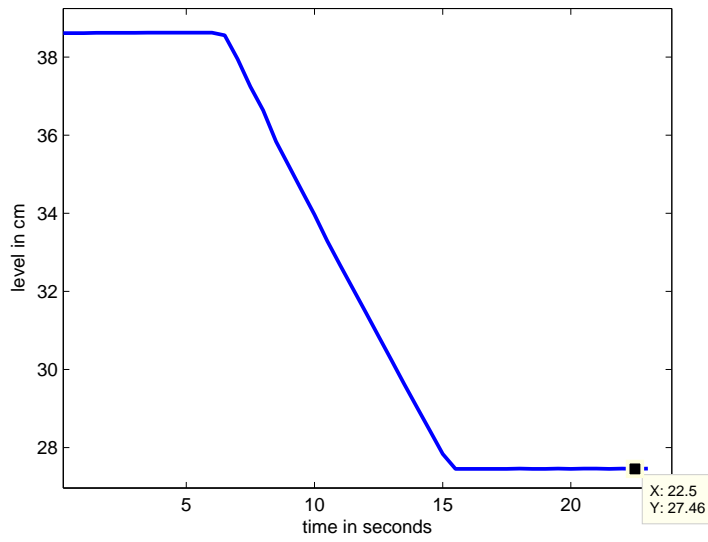
Figure 3.3: Draining liquid from the prototype

The decrease takes 20 measurements, i.e. 10 seconds, which corresponds to 1dL/s.

The decrease in level is linear and given as 1.12 cm/s.

This corresponds to $\sim$ 196 samples in adblue.

It is easy to see that averaging these two measurements will produce a result which will not be meaningful. However, if the trigger time was reduced considerably, it may be possible to achieve consecutive measurements in which the phase shift between these are small enough that averaging produce a meaningful result.
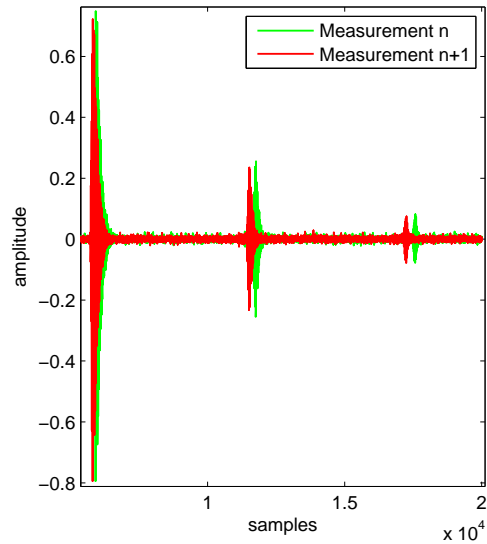
Figure 3.4: Two consecutive measurement in the draining test.

Although, as can be seen from equation 2.21, the mass flow from the pipe is dependant on the area of the hole. Thus it is possible to control the mass flow out of the pipe. In addition, the interval between measurements can be lowered to an absolute minimum by letting the time interval between triggers be as small as possible. This will again lead to the measurement being closer in time, and therefore more resembling as for averaging to function properly.

3.2.3 New prototype and temperature changes

The new prototype consists of a pipe with a transducer attached at the bottom, similar the previous prototype presented in [5]. However, this pipe is now fastened onto an adblue tank which is suited for vibration tests. These tanks have a slot for a urea quality-sensor in which the prototype pipe can be fitted. However, as the temperature changes are generated by pumping a coolant through a quality-sensor, and the slot for the quality sensor is occupied by the prototype pipe, it is not possible to combine these two. Therefore, temperature changes are simulated by pumping bubbles into the fluid. This is a reasonable simplification, as the main challenge for temperature changes in term of level measurement is that bubbles are generated in adblue as temperature increases.

3.3 Echo amplitude in pipe

When conducting experiments with the prototype, the amplitude of the returning echo seemed to vary with the liquid level. Transmission loss for a circular piston transducer along the transducer axis is found from equation 2.10 and is shown in figure 3.5.
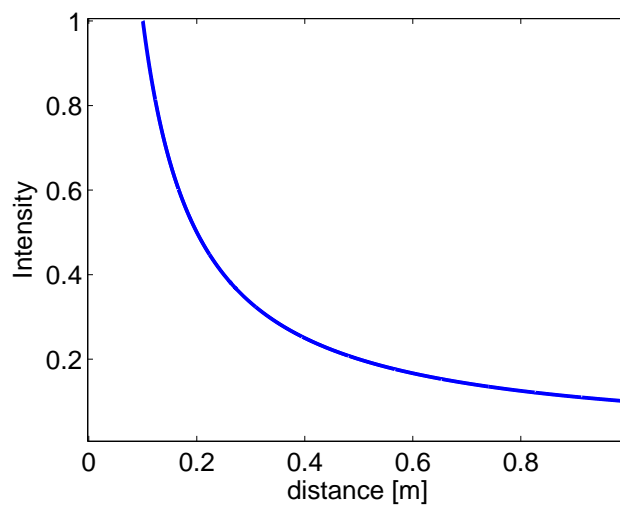
Figure 3.5: Spreading loss along the transducer axis

However, experimental data show
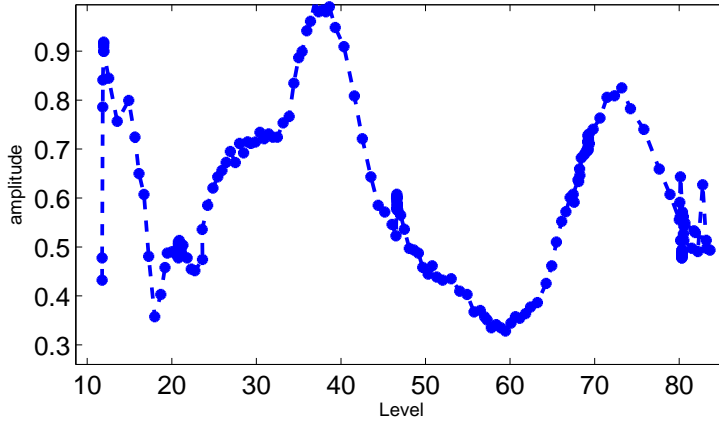
Figure 3.6: Normalized echo amplitude with 1 pulse at 1 MHz

As can be seen from figure 3.6, the echo amplitude as a function of level, varies significantly different compared to figure 3.5. Since the echo strength is a vital property of the measurement system, it is important to understand how it changes with the propagated distance inside the prototype pipe.

In light of this, a test plan is constructed with the following program:

	Trigger frequency $[MHz]$	Number of pulses	Length $[cm]$
Test set 1	0.58	1-4	15 - 95
Test set 2	1	1-4	15 - 95

The lengths were given as each 15 cm from 15 to 90 cm. For each length, a trigger with 1-4 pulses were applied. These tests were performed for both resonance frequencies.

3.4   Ultrasound simulation

During experiments studying the amplitude of the returning echo at different levels in the prototype, it was discovered that the signal strength of the returning echo varied in a non-intuitive manner. Since one of the main challenges with ultrasonic signals is the returning wave's amplitude, it is important to try to understand this phenomena and why it occurs. It was therefore decided to implement a model of the system in software to simulate the system. As the simulation in 3D with equations such as 2.2 is very memory consuming for systems of relatively large proportions (as this system), a 2D was used to try to provide an idea as to what happens with the amplitude of the ultrasonic as it propagates through a pipe. The idea was that if a model that could provide similar results as to what was observed in practice, the radius of the pipe could be changed and further simulations could provide give an indications of which radius would be optimal to use in terms of received signal amplitude.

3.4.1   Choosing a simulation tool

The possibilities of finding suitable simulation environments for the system was investigated. The choices narrowed down between COMSOL Multiphysics [10], a 3D physics simulator with possibilities of ultrasonic wave propagation and reflection, and the Matlab open-sourced toolbox K-wave, which contain a substantial framework for ultrasonic simulations.

Even though COMSOL Multiphysics seemed to provide a more extensive environment, the choice landed upon K-wave as the author had knowledge of Matlab, and the process to understand and use the COMSOL software was deemed to be too time consuming. K-wave is also open source, which meant that the development could start without requiring any licence.

3.4.2 K-wave

When simulating ultrasonics using methods such as finite element [11], many interesting problems require huge amounts of memory and computational time. The K-wave numerical model based upon the solutions of the following equations

$$\frac{\partial \mathbf{u}}{\partial t} = -\frac{1}{\rho_0} \bigtriangledown p \tag{3.1}$$

$$\frac{\partial \rho}{\partial t} = -\rho_0 \bigtriangledown \mathbf{u} \tag{3.2}$$

$$p = c_0^2 \rho \tag{3.3}$$

where $\mathbf{u}$ is particle velocity, p is acoustic pressure, and ρ is density.

By solving these equations using a k-space pseudo-spectral method [12], less memory and computational time is required compared with finite element methods and finite difference methods.

Using K-wave

K-wave was installed and by studying the provided examples a model resembling the actual system was developed. An important side note is that

k-wave toolbox was originally developed to simulate ultrasonic applications in medicine, as described to be able to simulate realistic behaviour in tissue-realistic media [13]. This did provide some challenges as to implementing a drastically different ultrasonic simulation.

2D vs 3D simulation

In order to achieve as much similarities between the actual system and the simulation model, a 3D simulation would have achieved the most realism. However, the decision landed on implementing a 2D model first to test if it was possible to simulate in two dimension. As the k-wave toolbox is primarily used for medical ultrasonic applications (which typically have smaller physical systems than the system presented in this paper), it was not known whether a 3D model would be possible to run with the given computational resources. This decision proved to be vital as the computational time and resource demands were of a large magnitude even for a 2D simulation. The two largest deciding factors for computational time and memory is the size of the computational grid and the simulation time step.

Computational Grid

When simulating an ultrasonic wave passing through a medium, one needs to define the medium into discrete elements. In a 2D simulation, the grid is composed of a number of points the x direction and in the y direction. Finite element methods can often require 10 grid points per wavelength to achieve adequate accuracy, while k-wave needs only 2 points per wavelength. Thus, when simulating a pipe with a 1m length, and a wavelength of $1.63mm$, at ten points per wavelength finite elements methods would require ca 6000 points in the x-direction, while k-wave only needs around 1200 points.

Depending the number of points in the computational grid, the grid has a maximum frequency that it can represent. The following formula can be used for calculating grid spacing

$$d = \frac{c_{min}}{n f_{max}} \tag{3.4}$$

where c_{min} is the minimum sound speed in the computational grid, n is the number of grid points per wavelength,and f_{max} is the maximum frequency the grid can represent. Due to Nyquist theorem n has to be at least two, i.e. $n \geq 2$, as to be able to represent a propagating wave in the grid.

After calculating the spacing between grid points with equation 3.4, the number of grid points needed can be found

$$N = l/d \tag{3.5}$$

where l is the length in meters. In this system a frequency of at least 1 MHz is required, and the maximum length is 1 meter. Seen from equation 3.4, the minimum sound speed in the system is of great importance. If a layer of air is used as a reflective surface in the system, where $c_{air} = 334\frac{m}{s}$, the grid spacing becomes smaller and thus more grid points are needed for a length of 1 meter. However, if a reflective surface made of steel is used, which has a sound speed of $c_{steel} = 6000\frac{m}{s}$, c_{min} becomes that of adblue at around $1630\frac{m}{s}$. Since a plate of steel is the reflective surface of the floater, this choice will be most realistic when comparing the simulation with the actual data made in the lab. It should be noticed that a reflective surface of air was not possible on the computers accessible to the author, as Matlab ran out of memory with the number of grid points needed to have a reflective surface of air. More information regarding the computational grid can be

found in the k-wave user manual [14], as well as equation 3.4 and 3.5.

Simulation time

The simulation requires some way to keep track of time, i.e. decide at which
instances to solve the equations 3.1 - 3.3. The time-step decides how much
time it is between to such calculations. The time-step needs to satisfy the
equation

$$dt = CFL\frac{d}{c_{min}} \tag{3.6}$$

where d is the grid spacing found in equation 3.4, c_{min} is the mini-
mum sound speed in the heterogeneous medium, and CFL is the Courant-
Friedrichs-Lewy number.

The time step dt can be a decisive factor in both numerical stability and
also accuracy in the model. The CFL "is defined as the ratio of the distance
a wave can travel in one time step to the grid spacing." [14]. It is noted
that a CFL of 0.3 provides balance between accuracy and computational
speed. For the simulations in question which are heterogeneous, this was
guaranteed to ensure stability. It is however not necessarily small enough
to guarantee accuracy. The recommended method was to decrease the time
step until the simulation result for a given scenario did not yield different
results. After running the simulations with the recommended CFL of 0.3,
and noticing that reducing it further resulted in a computational time that
was rather high, or even out of memory errors, the CFL was kept at 0.3.
This resulted in a computation time of Ca. 6 hours.

Defining the medium

The medium in the system is made up of four parts

1. PML

2. Plastic pipe

3. Reflective steel plate

4. Adblue

For all grid points in the computational grid, density and speed of sound has to be defined. The actual density and speed of sound for the plastic pipe was not known, as even for a given type of plastic like PP or PE, such values differ a lot between manufacturers. Factors like how porous the material is, density of the plastic and speed of sound can vary. Thus values were found through some guidance from [15]. As the reflections from the simulation provided similar results as what was seen in the actual experiments, these value was chosen for all the simulations. As for the steel plate, values were provided by Wema. The acoustic impedance should provide a theoretical reflection as shown in [5], so these values provided a reflection that was studied and deemed to be sufficient. The values for density and speed of sound in adblue are well known. The values chosen in the simulation were consistent with adblue in room temperature. Thus the values chosen were:

	Speed of Sound $[\frac{m}{s}]$	Density $[kg/m^3]$
Plastic Pipe	2200	1200
Steel Plate	6000	7700
Adblue	1630	1087

PML stands for Perfectly Matched Layer. The PML is layer that encloses the computational grid. Its main purpose is to absorb waves that travel beyond the grid. The absorption value and size of the PML were factors that was altered from the default settings provided by k-wave. The PML absorption in 2D simulation is a vector containing two values: one for each of the two dimensions. It is especially important that the direction perpendicular to the transducer surface, i.e. the way the wave is travelling in, has a high PML-absorption. The reason why this is important is because in k-wave, waves that travel beyond the PML will reappear at the opposite side of the domain. When sending the transducer pulse from one end of the pipe, it is vital that no part of the wave would travel through the PML and reappear behind the reflection plate. Therefore, the PML-absorption value in said direction was set to be relatively high. The combination of a high absorption value and an increased PML size, meant that no energy was observed to reappear at the other side of the domain. The increased PML size meant that the wave would have to travel through a larger grid with a high absorption value, which means that the total absorption increased.

The final values chosen for the PML were 2 $\frac{nepers}{gridpoint}$ in both x and y direction. Initially, before the inclusion of the plastic pipe in the model, the PML absorption in y-direction was set to 0. This meant that the waves passing through the domain in the y-direction would reappear on the other side, i.e. total reflection in the y-direction. To make the model more realistic, the plastic layer was added and the PML was set to the default value, as the reflection between the plastic layer and the adblue layer would be sufficient to account for internal reflections inside the pipe.

Absorption

K-wave models absorption in the following way

$$\alpha = \alpha_0 \omega^y \tag{3.7}$$

where α is the absorption coefficient, ω is the angular frequency, and α_0 and y are material dependent coefficients, with $1 < y < 2$. K-wave only allows for a single absorption coefficient that is scalar, and not defined for each media in the system. Therefore, simulating a heterogeneous media combined with absorption is troublesome, as the different parts of the model in reality has varying absorption coefficients, while K-wave only allows a uniform coefficient.

The actual values for adblue in equation 3.7 is not known. However, since adblue consists of partially distilled water, it might be comparable to the absorption of distilled water. K-wave has a built-in function to calculate the absorption coefficient at a given temperature in distilled water, which are based upon the experimental work by Pinkerton [16]. K-wave uses a 7th order polynomial to create a continuous curve to fit the data provided by [16]. From this polynomial, it is clear that, for a ultrasonic signal with a frequency of 1 MHz, and assuming 25 degrees Celsius in the distilled water, $\alpha = 0.0019 \frac{dB}{cm}$. As this was deemed to not have a significant impact on the amplitude of the ultrasonic signal, it was decided that the absorption coefficient was set to zero for the entire model.

Defining an acoustic source

While equations 3.1-3.3 describes how a wave propagates, the wave needs a mechanism to be generated. Equations 3.1-3.2 can be written as

$$\frac{\partial \mathbf{u}}{\partial t} = -\frac{1}{\rho_0} \, \bigtriangledown \, p + \mathbf{S_F} \tag{3.8}$$

$$\frac{\partial \rho}{\partial t} = -\rho_0 \, \bigtriangledown \, \mathbf{u} + \mathbf{S_M} \tag{3.9}$$

Where $\mathbf{S_F}$ is an force source term given in $\frac{N}{kg}$, and $\mathbf{S_M}$ is a mass source term in $\frac{kg}{m^3 s}$. The most important difference between mass and force sources, is that force is a vector, while a mass source radiates equally in all directions. An actual transducer is providing a volumetric change in the piezoelectric element as a result of the applied voltage. It is therefore a mass source. However, since a transducer is directional, a standard mass source as provided by k-wave will radiate in all directions. It was shown through equation 2.12 that the transducer in this system has a beam-width of $\approx$ °11.9. K-wave has support for the implementation of transducers, where properties such as directivity can be added. However, this is only supported in 3D.

To achieve a simulation which resembles reality as much as possible, the source can be placed close to the edge of the computational domain. This ensures that parts of the wave that are undesirable, will propagate into the PML and deteriorate. The obvious position for the source is at the end of the domain that corresponds to the bottom part of the pipe. Since the part of the wave that travels in the negative x-direction as shown in (3.7) is found to be be absorbed by the PML through simulations, it will not reappear at the other side of the domain. However, it is not possible to achieve a beam-width of $\approx$ °11.9. In the simulations, part of the wave travelling in the positive and negative y - direction is reflected back against the source. This is unfortunate as the source position is the same as the sensor position. (since the system sends and receives with the same transducer).

To compensate for the equal spread in all directions by the source, it is possible to define sensor directivity in K-wave. By defining the sensor directivity to be in the x-direction, the returning wave from the plastic wall along the same x-position as the sensor, the energy will not be sensed by the sensor and thus will not effect the result of the simulation. It is not possible as of yet to define transducers with directivity functions as described by equation 2.9 in 2D in k-wave.

An example of the finished grid with a propagating pulse is shown in figure 3.7.
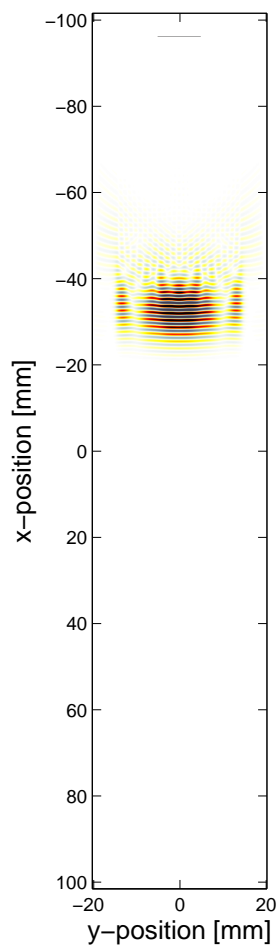
Figure 3.7: Simulation example

3.5   Modifying the bandpass filter

As the filter that is on the PCB amplifies the two resonance frequencies with different magnitude, it is of interest to modify the coefficients in the bandpass filter and study the effect this has on the ultrasonic signal. The filter on the PCB as of now has a theoretical magnitude response as shown in 2.6. Experiments have shown that trigging on the lowest resonance frequency can increase the energy of the returning echo, which is vital to achieving a successful level measurement. Thus, a magnitude response that amplifies both resonance frequencies with a equal magnitude is desirable to investigate. To achieve this one has to modify the filter coefficients found in equation 2.16 - 2.16. However, since changing the filter components on the PCB is a time-consuming operation, it was decided that the best approach would be to find theoretical values for the filter coefficients that would give the desired magnitude response. This could be done by trying different values for the coefficients in the transfer functions in equations 2.16 - 2.16 and calculate the magnitude response. One problem with using the transfer functions for this purpose is that it does not account for non-ideal behaviour by the components. It was therefore recommended by Wema personnel that the circuit was tested in an electric circuit simulator such as LTSpice, to investigate the magnitude response.

3.5.1   Learning LTSpice

SPICE stands for Simulation Program with Integrated Circuit Emphasis. There have been many different SPICEs since the first simulator was developed at Berkeley in 1973 [17]. LTSpice is a SPICE developed by Linear Technology [18]. LTSpice contains an schematic editor that provides the user with drawings of circuit components that can be inserted into the circuit model. After the circuit is constructed the user has an overview of all the components with their respective values as shown in figure 3.8.
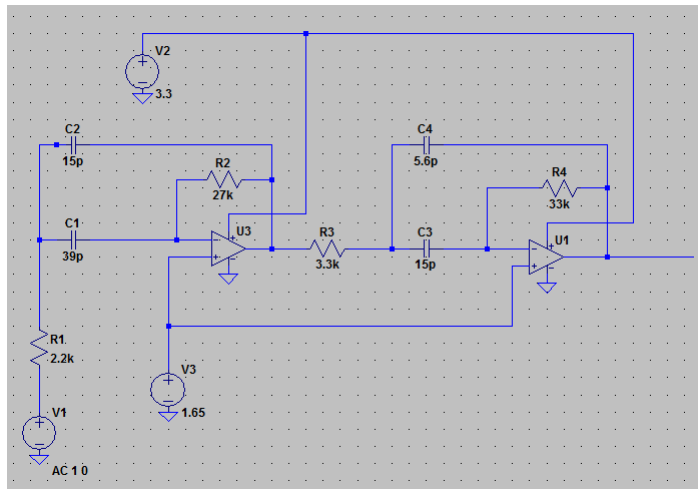

Figure 3.8: LTSpice schematic example

3.5.2   Finding new filter coefficients

Using LTSpice the filter circuit could be simulated to provide a more realistic magnitude and phase response of the filter than the responses provided

by the transfer function in section 2.7. By applying a simulator such as LTspice, assumptions such as an ideal operational amplifier can be replaced with realistic models made by the manufacturers of that specific amplifier.

The receiver circuit with the current values was implemented in LTspice and simulations were made. The magnitude- and phase response are shown in figure 3.9.
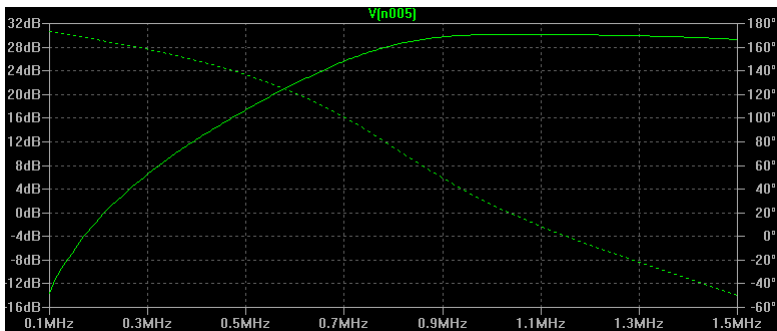

Figure 3.9: LTSpice bode plot for todays receiver circuit

In order to expand the bandpass of the filter, a Matlab script were made to calculate different magnitude responses. Suitable values for the filter coefficients were found. The new values were applied to the filter circuit in LTSpice and simulated.

As it would be time consuming to design a filter with a suitable magnitude and phase response, the phase response was not prioritized, i.e. there would be a certain phase shift for the resonance frequencies. The more interesting thing to study was how the magnitude of the lowest resonance frequency would look when amplified with the same magnitude as the higher resonance frequency. The bode plot for the new filter coefficients are shown in figure 3.10.
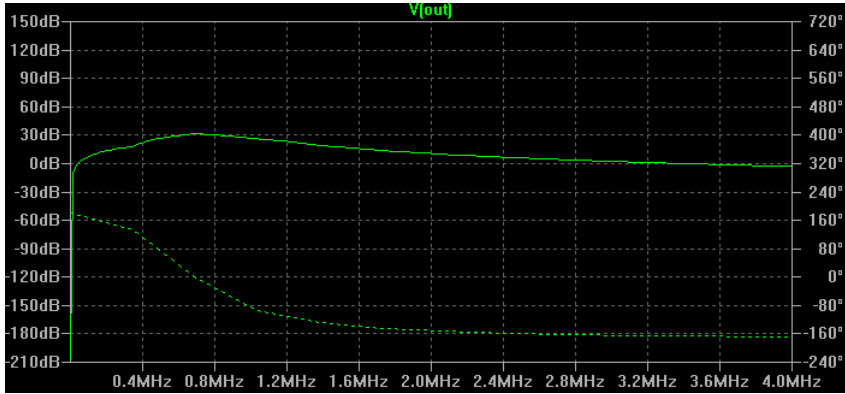
Figure 3.10: LTSpice bode plot for new receiver circuit

where the solid line is the magnitude response and the dotted line is the phase response. As can be seen from figure 3.10, there is a phase shift for both resonance frequencies, in opposite directions.

The new values for the resistors and capacitors were soldered onto a PCB and tests were made with 4 pulses at 1 MHz and 4 pulses at 580 kHz.

3.6   Pre-processing

The preprocessing consists of the same procedures as used in [5]. However instead of removing the startup-noise completely, the first 700 samples are simply set to zero.

In order for correlation to work, the signal needs to fluctuate around zero. Thus the signal is also normalized around zero.

3.7   Echo detection algorithm

The echo detection algorithm was updated from the previous algorithm as presented in [5]. The main purpose of this algorithm is to locate echoes in the measurement. The algorithm should return an index which is inside an echo, as to serve as a starting point when the echo start is to be detected.

The new proposed algorithm is dependent on the following properties of the ultrasonic echo from the floater:

1. Amplitude

2. Frequency content of 1 MHz

3. Frequency content of 580 kHz

The idea is to decide where the echo is based on the amplitude, correlation with 1 MHz and correlation with 580 kHz. The idea is that the amplitude will serve as to ensure that the located echo is containing samples which have values that deviates from the mean of the measurement. On the other hand, correlation is noise suppressing by nature, while also rewarding high value samples.

3.7.1   Amplitude

Regarding the property of the measurement related to signal strength, the energy measure that was used in [5]) is replaced with the amplitude. The property used in [5] was

$$E_n = \sum_{n-\frac{N}{2}}^{n+\frac{N}{2}} |x(i)^2| n = \frac{N}{2} \dots M - \frac{N}{2} \tag{3.10}$$

Where N is the size of the window used to calculate the formulae at position n, and M is the total signal length. This method produces a result which is well suited to find the echo(s) contained in the measurement. However, since the value of E_n is a sum of the surrounding samples in a window of size N, it is not really clear defined as an actual physical property. The standard amplitude is a measured voltage which translates to pressure, so it is more intuitive what the amplitude actually is, compared to the result of equation 3.8. In addition, equation 3.8 is non-linear compared to amplitude. If the amplitude of a sample is twice as big as that of another, the result from 3.8 might not be twice as big, depending on the values of the surrounding samples. Thus, changing to the amplitude will make for a more comparable property for the strength of echoes.

Amplitude envelope

The new formulae replacing equation 3.8 is given as

Algorithm 1 Amplitude envelope

> **for** $i \leftarrow 2, n - 1$ **do**
> > **if** $abs(m(i)) \geq abs(m(i - 1))$ **and** $abs(m(i)) \geq abs(m(i + 1))$ **then**
> > > $envelope \leftarrow m(i)$
> > > $indices \leftarrow i$
> > **end if**
> **end for**

---

where m is measurement and n is the number of samples in m. The array *indices* is used to store the indices of the values in *envelope*. The resulting envelope is shown in figure 3.11. The multiple echoes seen in the figure is a result of a diesel layer on top of the adblue.
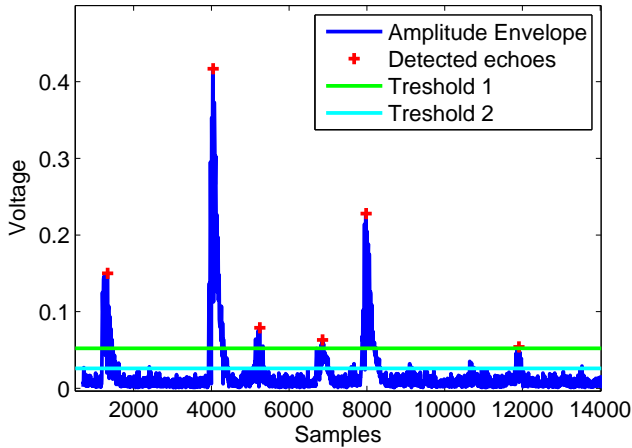
Figure 3.11: Amplitude envelope

For the envelope of the signal the interesting property is the energy contained in the measurement. A procedure for deciding if there is energy in the measurement which resembles the appearance of an echo is needed. One way to achieve this is to have threshold in which the signal need to surpass with at least a group of samples in close vicinity of each other. If this found in the envelope, it is likely that there is an echo in this location. To make sure that multiple echoes can be detected, one can detect locations in the measurement that have multiple consecutive values which are close to the mean of the signal. Such a location will not be inside an echo. If one demands such a location between two echoes, it is possible to separate between echoes, and not make any value which is above the threshold an echo. An example can be given from figure 3.11. If the green line is surpassed, an echo candidate is detected. This candidate is only confirmed as an echo if there is a location between the new candidate and the previous

echo which is below the cyan line.

By using this approach, the algorithm does not force an echo to have many consecutive peaks which are above the threshold. By looking at the echoes left and right of the 6000 sample mark, one can see that these echoes do not have as many peaks above the green line as for instance the main echo has. Thus small echoes can be detected by not enforcing a large number of peaks that are above the green line. However, this also makes the algorithm vulnerable to high amplitude noise.

The implementation contains two threshold values:

- T_1: A threshold that decides the location of an echo. If this threshold is surpassed, it is decided that there is an echo at this location. The maximum value within a vicinity of σ values of the envelope. This index is then stored as an echo location. T_1 is calculated as a factor of the maximum value of the measurement, that is $T_1 = \alpha M$ where M is the maximum value of the entire measurement.

- T_2: A threshold used to decide when an echo ends. If γ consecutive values of the envelope are below this threshold, the echo has ended. It follows that $T_1 > T_2$ if any echoes are to be detected. Thus to make the T_2 scale with T_1, T_2 can be chosen as $T_2 = \beta T_1$, where $\beta < 1$.

The echo detection procedure is given in algorithm 2.

Algorithm 2 Echo finder

$echoes = 0$
$end_{ind} = 0$
for $j \leftarrow 1 + \gamma : n - \gamma$ **do**
    if $envelope(j) > T_1$ **then**
        if $size(echoes) == 0$ **then**
            $echo_{max}, echo_{ind} = max(envelope(j : j + \sigma))$
            $MAX_{echoes} \leftarrow echo_{max}$
            $MAX_{indices} \leftarrow echo_{ind}$
            $echo_{last} \leftarrow echo_{ind}$
        else
            if $end_{ind} > echo_{last}$ **and** $end_{ind} < envelope(j)$ **then**
                $echo_{max}, echo_{ind} = max(envelope(j : j + \sigma))$
                $MAX_{echoes} \leftarrow echo_{max}$
                $MAX_{indices} \leftarrow echo_{ind}$
                $echo_{last} \leftarrow echo_{ind}$
            end if
        end if
    else if $envelope(j) < T_2$ **then**
        for $k = j : k + \gamma$ **do**
            if $envelope(k) > T_2$ **then**
                break
            end if
        end for
        $end_{ind} = k$
    end if
end for

The first time the algorithm finds a value that is larger than T_1, it registers an echo. When it finds a new candidate after the first, it only registers an echo if there has been an $echo_{end}$ between the new candidate and the previous echo. The entire procedure is reliant of the following constants:

1. α - defines the threshold $T_1 = \alpha M$ where M is the maximum of the measurement.

2. β - defines the threshold $T_2 = \beta T_1$

3. γ - number of consecutive values that must be below T_2 to update $echo_{end}$

4. σ defines how many elements that is included in the set where the maxima is searched for after T_1 is crossed.

γ essentially defines how many consecutive values below T_2 there should be between two echoes for both to be detected.

σ is related to how many peaks that should be checked for the maximum, since the envelope contains only the echo peaks. Since the echo maximum typically is one of the first five peaks, the most important factor is that it is not set too high as to start searching in another echo that is close in RTT as the echo that has been detected.

α and β however are more important factors, and are vital to the performance of the algorithm. In order for the algorithm to work, $\beta \leq \alpha$ needs to be enforced, or else the end of an echo could be located inside what is believed to be an echo. Also, as a requirement for an echo detection is that T_1 is crossed, α cannot be to low as to detect low amplitude noise as echoes.

The amplitude of the echo will vary with the distance to the surface, and therefore the amplitude itself is of a too varying nature as to decide where the main echo is. Although the main echo normally possesses the maximum of a measurement, it might still be hard to separate echo from noise when the signal strength is low.

The algorithm now have dynamic values for the thresholds, and will adapt to the echo strength from measurement to measurement. Another option would be to have hard coded values for these thresholds. This option is not tested in this thesis, and would likely have to based on large amounts of recorded data under varying settings regarding levels and noise. This also applies for the parameters α and β used in the algorithm. Thus the parameters are set in this report without any statistical justification. The values were chosen by trial and error.

3.7.2 Correlation

The main advantage of correlation is that it is able to find echoes by looking for a given frequency in the measurement. Since the piezoelectric element has two resonance frequencies, it is decided to correlate with a pulse of each resonance frequency.

The algorithm in [5] also contained correlation. However, it only correlated with a 1MHz pulse. Since the tests in this thesis compared to [5] have triggers of both frequencies, and contain more noise, correlating with the two frequencies is done as to study whether one frequency might not be dampened away by noise in the form of bubbles. It is therefore proposed to correlate with both resonance frequencies. An additional change is that a toneburst is used instead of a 1 MHz pulse with a constant amplitude. An example is shown in figure 3.12

The correlation result resembles the actual measurement, meaning it has a clear "echo" where the correlation between the actual echo and the toneburst occurs. Since the basic structure in the correlation and the envelope of the signal are the same, the algorithm employed to detect an echo can be used for the correlation as well. However, since the correlation is scaled in a different manner than the amplitude, it is necessary to change the constants the algorithm relies on. There can also be a difference between the correlations regarding what values that should be used for the constants.

Figure 3.12 is an example of an ultrasonic echo correlated with a toneburst pulse
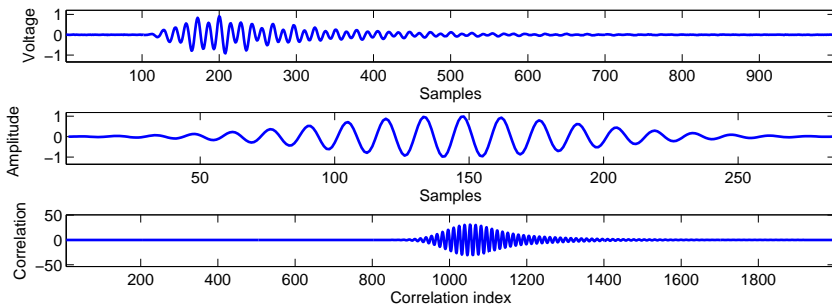
Figure 3.12: Example of correlation

3.7.3   Combining the results

After a measurement has been pre-processed, the amplitude and correlation procedures have detected an index in which the echo is located. If all the methods agree on an echo location, (within a certain deviation), than it is

safe to say that an echo is located at this location. However, under the presence of noise, one or two of the methods might fail, or disagree. It is therefore necessary to combine the results from the three methods in some way that will yield a high certainty that the resulting echo location(s) are correct. This is solved in this thesis by declaring that if two methods agree on a location, it is confirmed as an echo location.

3.8 Detecting the echo start

After an echo has been detected and an index inside the echo has been located, the next step is to detect the start of the echo. In [5] this was done by back-tracing the energy property as defined in equation 3.10, until the energy was under a certain limit. As the desire for increased accuracy presents itself, a new procedure for finding the echo start is proposed. It is assumed in this procedure that the echo locator has found an index inside the echo. The proposed approach is to back-trace the signal sample by sample until the echo start is detected. The method is given as follows:

The algorithm stores all the peaks that have the correct frequency, which is defined to lie inside the interval $[min\_freq, max\_freq]$. The peaks with the correct frequency that also has an amplitude larger than min_ampl are stored in $peaks$. The last peak that is stored before the index i has reached $echo_{index} - \zeta$ is determined to be the start of the echo.

The algorithm relies on the parameters

- min_freq

- max_freq

Algorithm 3 Echo start finder

$i \leftarrow echo_{index}$
$peaks \leftarrow 0$
$last\_peak = 0$
while !($echo\_start\_detected$) **do**
   $i = i - 1$
   if $abs(m(i)) \geq abs(m(i-1))$ **and** $abs(mt(i)) \geq abs(m(i+1))$ **then**
      if $size(peaks) == 0$ **then**
         $peaks(last\_peak) \leftarrow i$
         $last\_peak = last\_peak + 1$
      else
         if $peaks(last\_peak)$ $-$ i $\leq$
max_freq **and** $peaks(last\_peak) - i \geq min\_freq$ **then**
            if $m(i) > min\_ampl$ **then**
               $peaks(last\_peak) \leftarrow i$
               $last\_peak = last_peak + 1$
            end if
         end if
      end if
   end if
   if $echo_{index} - i \geq \zeta$ **then**
      break
   end if
   $echo\_start\_index = peaks(last\_peak)$
end while

- min_ampl

- ζ

The interval $[min\_freq, max\_freq]$ can be found using the formula

$$s_m = \frac{f_s}{f_m}, m = min, max \tag{3.11}$$

where f_s is the sampling frequency, f_m is the actual frequency of the signal, and s_m is the number of samples in a period of that frequency. Since all peaks are stored, both positive and negative, the values for min_freq and max_freq should be equal to $\frac{1}{2}s_{min}$ and $\frac{1}{2}s_{max}$, respectively. It is also important to make the interval slightly bigger than the values found for s_{min} and s_{max} since the sampling frequency is not an integer. This might lead to that a period of the same frequency might have +1/-1 sample.

The parameter min_ampl is the lowest amplitude possible for a peak to be registered, and is therefore important to the performance of the algorithm. It is calculated as $min\_ampl = aM$, and is therefore adjusted from echo to echo.

ζ decides how many samples that is included in the backtracking before the algorithm stops. It is important not to stop before the echo is considered over. Also there might be other echoes in the measurement that have arrived prior to the one in question, and this ζ should terminate the search for the echo start before another echo is encountered.

The reason for including the possibility of an echo located anywhere in the measurement, is the detection of diesel layers. With only one fluid medium in the tank, the echoes should appear with the same distance between them. However, with multiple fluid layers, echoes can appear anywhere in the measurement, depending on the thickness of the layers.

3.9   Discarding measurements

A measurement is discarded if the variance of the measurement is less than
a certain threshold. The formula for variance can be found in equation
2.25. Variance can be used as a measure of echo strength. As can be
seen from 2.25, an measurement containing a strong echo will have more
samples which are significantly distant from the mean value of the signal.
A measurement in which the echo is weak or non-existent however, will
have a significantly lower variance. Thus a measurement is discarded if a
measurement x fulfils the requirement $Var(x) < T_3$. An example from a
measurement with various noise conditions can be seen in figure 3.13
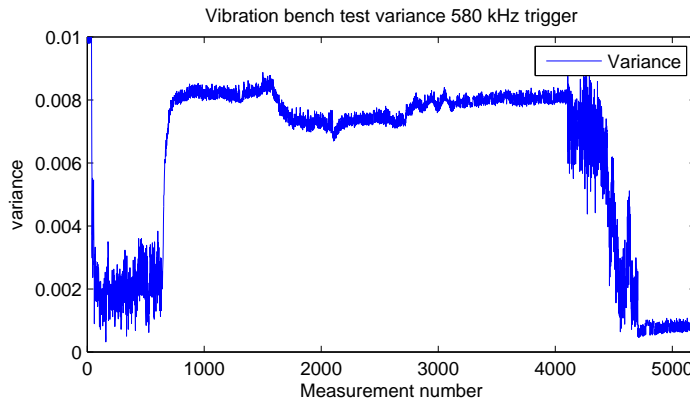
Figure 3.13: Variance of a dataset containing vibration

As can be 3.13, the start and end of the dataset contain measurements
with very low variance. The variance limit set for discarding a measurement
were 0.001 for all tests. This value was chosen by trial and error, as it is in
the proximity of this value that the echo is almost not visible to the human

eye.

3.10 Vibration tests

As stated in the problem description, the system is to be tested under
the stress of vibration, in order to see how this affects the ultrasonic signal.
Wema possess a vibration bench which can be used to create vibrations with
a desired frequency. However, it was clear that the current prototype would
not endure the vibrations created by the vibration bench. It was therefore
necessary to create a new prototype that could contain the liquid without
spilling it when vibrating, as well as a pipe with a transducer mounted at
the bottom of it. It would also need to have such a shape that it could
easily be mounted on the vibration bench. A picture of the vibration bench
with the prototype mounted on it can be seen in 3.14.
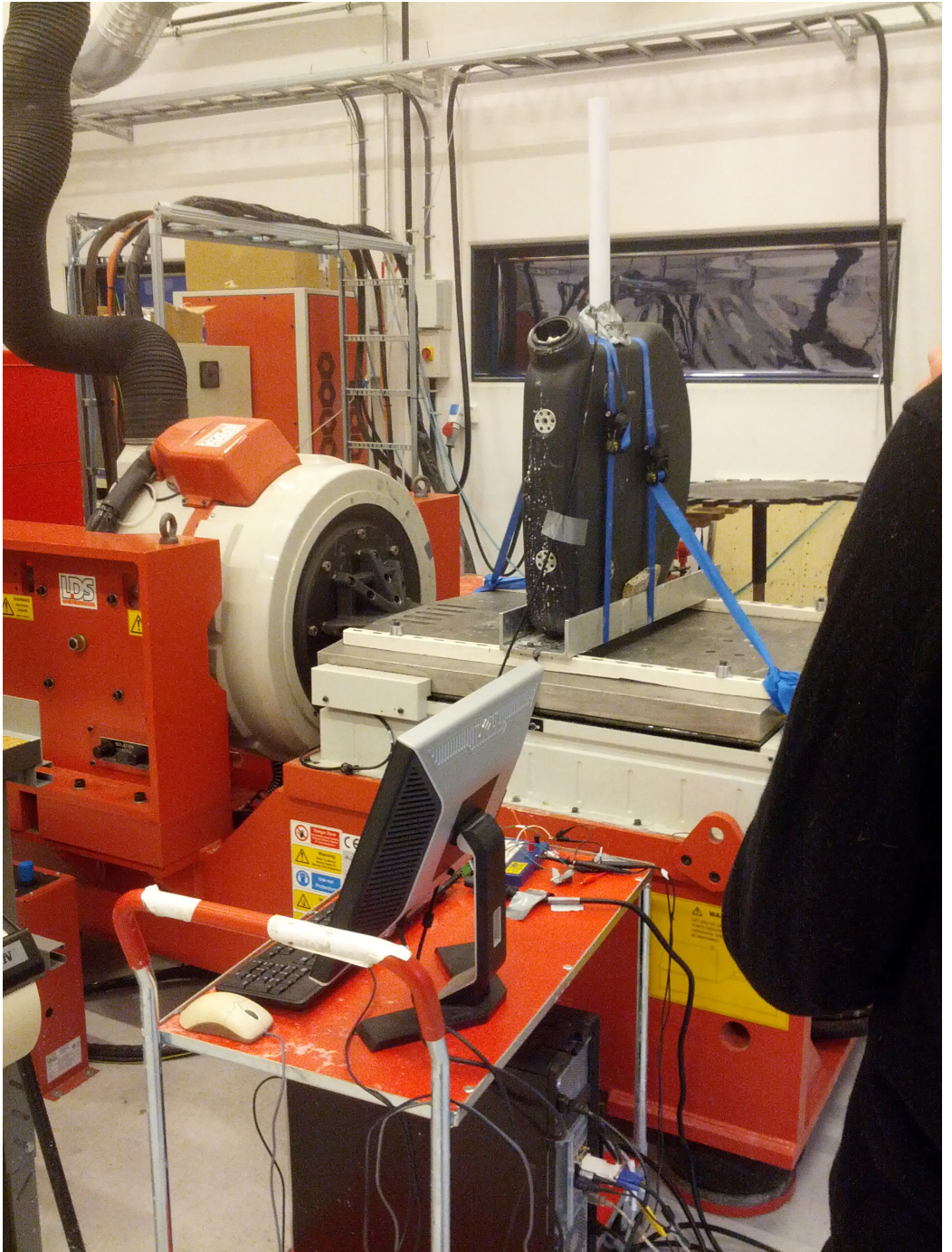
Figure 3.14: Vibration bench setup

Test program

The vibration test program used in the tests were recommended by Wema personnel, as the vibration frequencies are chosen to resemble different types of diesel engines. The program consists of the following parts:

	Frequency $[Hz]$	Duration $[min]$
Part 1	10	15
Part 2	15	15
Part 3	40	15
Part 4	5	15

In addition, there is a break when transitioning to the next phase in the program. Since the phases have to be started manually, there are small variations in how long the breaks between phases are.

Triggers

Three different triggers were chosen as to test the effect of the trigger as resistance to noise:

	Frequency $[MHz]$	Number of pulses	High - low time $[\%]$
Trigger 1	0.58	4	50 - 50
Trigger 2	1	4	50 - 50
Trigger 3	1	4	30 - 70

High - low time corresponds to how much of a period the pulse is high and low, in percentage. The triggers programs are generated as described by section 3.1.2.

As a trigger is applied and a the corresponding measurement is recorded, there is a break of 0.5 s between the time a trigger is applied to the next trigger is applied. This is as to ensure that the piezo and the measurement system is at rest when the next trigger is due.

3.11 Diesel layers

As previously mentioned, it is desirable to explore how a mixture of diesel and adblue will effect the ultrasonic signal.

Since the density of diesel is less than the density of adblue, diesel will form a layer on top of the adblue. Also, a floater made to float in adblue, such as the floater used in the experiments, will not float in diesel. This can be seen from section 2.9 and section 3.2.1. The tests performed with diesel poured on top of the adblue where conducted without a floater because of this.

The fluid properties for the three medias involved are

	Speed of Sound $[\frac{m}{s}]$	Density $[kg/m^3]$
Adblue	1630	1087
Diesel	1350	832
Air	334	1.2

The reflection coefficients involved in the propagation of the ultrasonic wave can be calculated using equation 2.23 is therefore

- $R_{adblue-diesel} \approx -0.22$

- $R_{diesel-air} \approx -1.0$

- $R_{diesel-adblue} \approx 0.22$

The negative sign of the coefficients means that the reflected parts of the signal will be phase shifted. Therefore, 22 % of the propagating acoustic energy will be reflected as the wave is transmitted into the diesel layer. Thus the part of the wave that is reflected at the adblue-diesel, will be the first echo received by the transducer. All the remaining energy will be reflected at the diesel-air interface. As the wave propagates back to the diesel adblue interface, the wave will again be reflected at the diesel-adblue interface by a factor of 0.22 and the rest will propagate into the adblue and be received by the transducer as the second echo. See figure 3.15.
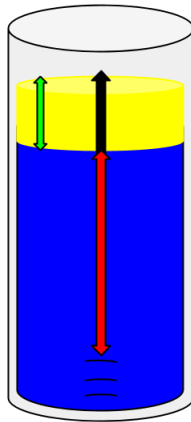
Figure 3.15: Diesel-Adblue layers demonstration

Depending on the thickness of the different layers, the returning echoes can be from different interfaces. If the adblue layer is significantly thinner

than the diesel layer, the echo travelling from the transducer and to the
adblue diesel interface (as indicated by the red arrow in figure 3.15), can
travel back and forth multiple times before the echo from the diesel air
interface (indicated by the black arrow in figure 3.15) returns.

A measurement from the diesel experiments can be seen in 3.16. As pre-
dicted by the theoretical reflection coefficients, the second echo is stronger
than the first echo. As the energy is reflected inside the diesel layer, more
echoes will be travel back to the transducer, though with deteriorating
strength.
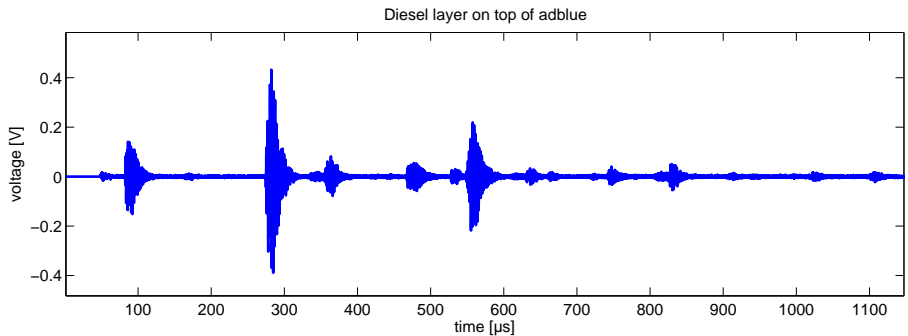
Figure 3.16: Diesel layer on top of adblue

In this measurement, the first echo is from the adblue-diesel interface.
The second echo is from the diesel-air interface. The third echo is the
remaining energy from the adblue-diesel interface which has travelled first
the red arrow in figure 3.15, and then the black arrow in 3.15. The forth
echo is a remnant of energy of the main echo in the measurement (from the
diesel-air interface) which has travelled up the black arrow, and then the
green arrow, and back again to the transducer. Depending on the thickness

of the different layers, these echoes (the third and fourth in the example), can switch places.

By inspecting these measurements, a pattern emerges. As the reflection coefficient of the diesel-air interface is larger than the adblue-diesel interface, the first echo might not be the strongest echo. Secondly, the echo appear not periodically in relation to arrival time.

Therefore, the echo detector as described in 3.7 might be used to detect the presence of additional liquid layers. By studying the echo locations and the signal strength in each individual echo, the presence of the diesel layer might be detected.

3.11.1 Diesel tests

The purpose of conducting experiments with diesel on top of adblue is to search for properties that are unique for the layering of the liquids.

Two different approaches are specifically studied:

- The properties of the multiple echoes that arises due to the extra interfaces between the liquids.

- The frequency content of the echoes that have propagated through different layers.

Tests were performed in the following manner. Diesel was poured into the prototype, which already contained adblue. By lowering the prototype pipe into the adblue "tank", the adblue level could be raised with the diesel still in top. The tests contained these scenarios:

	Total level[cm]	Diesel Added[dL]
Test 1	15	3
Test 2	30	3
Test 3	45	3
Test 4	60	3

Every test was performed with both a trigger with 4 pulses at 1MHz, and a trigger with 4 pulses at 580 kHz.

Chapter 4

Results

4.1   Echo amplitude

The following data are the results of the test plan presented in chapter 3.3. The experiments were executed to illustrate the change in signal strength as a function of the level in the prototype pipe.

It is clear from figures 4.1 - 4.2 that the signal strength is a function of frequency, the level in the prototype, and the number of pulses in the trigger. Also, the 580 kHz trigger is seen to be overall better performing regarding as to the echo amplitude compared to the trigger of 1MHz.
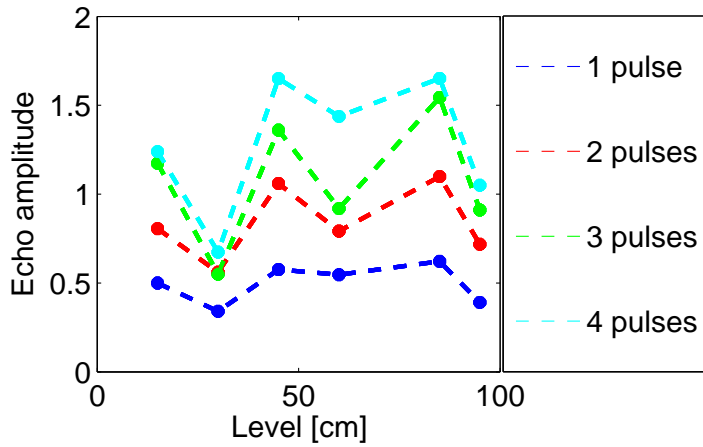
Figure 4.1: Echo amplitude in prototype with 580 kHz trigger
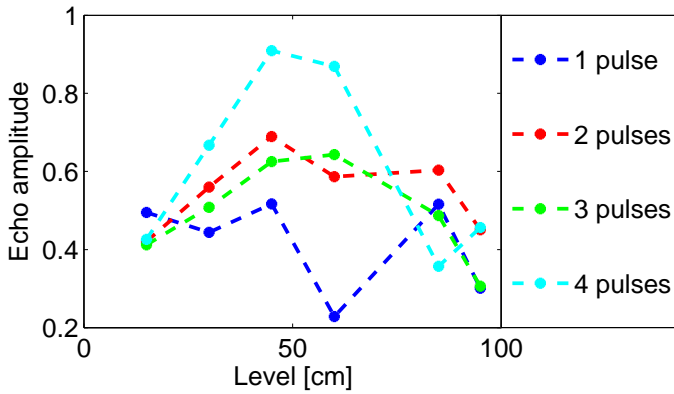
Figure 4.2: Echo amplitude in prototype with 1MHz trigger

4.2 Simulator results

As the signal strength of the returning ultrasonic wave is vital to the level measurement system, it is desirable to understand how the echo amplitude changes with different levels of liquid in the tank. Based on the results shown in chapter 4.1, a simulator was implemented as described in chapter 3.4. Simulations were made for levels from 0.1 m to 1 m with a spacing of 10 cm.

The results of the simulation data compared with the experimental data are shown in figure 4.3. Note that both the simulation and the experimental results have been scaled as to be comparable. This is due to the fact that the simulation outputs units of Pascal, while the experimental output is Voltage.
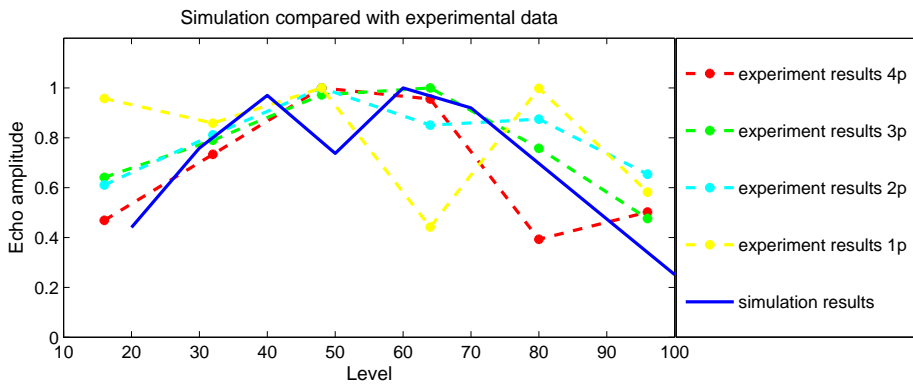
Figure 4.3: Simulation compared with experimental data

From figure 4.3 it can be seen that the simulation results have a similar shape in echo amplitude compared with the experiment results. The ultra-

sonic pulse length, which is proportional to the number of triggers in the experimental data, seem to have significant impact as to how the amplitude varies with the level.

4.3   Vibration

The test program as described in chapter 3.10 were performed for three different liquid levels in the prototype. A small dataset was made before each test as to calculate the correct level based on a measurement without noise. These levels were found to be 16.2 cm, 31.92 cm and 39.6 cm. Out of the three triggers that was applied to the transducer, the trigger with a frequency of 580 kHz proved to give the least discarded measurements and overall best performance. Also the 5 Hz and 10 Hz frequencies in the vibration program seem to be the most difficult phases in the tests as to measure the level successfully. It should also be noted that different frequencies are less difficult at certain levels, and increasingly difficult at other levels. Regarding accuracy as to the actual level in the measurements, it should be noted that these results were not produced to compare accuracy. This is because the procedure that searches for the echo start as given by algorithm 3 lacks the necessary tuning of the algorithm parameters as to perform well in an accuracy test. Also, the fact that three different triggers were used with a relatively big time-jump between them makes averaging unsuitable for these tests. Since the tests also contain higher noise levels in the form of electric noise, detecting the correct start of the echo will be even more difficult for the echo start finder. The goal of these tests are therefore to find which trigger is best suited in terms of signal strength. Accuracy is still compared to introduce a sense of how the algorithm performs.

Since the programs were started manually, it is difficult to know exactly

when a new phase in the tests starts. The following figure can be used as a guideline for how the dataset is produced. A large number of out layers or discarded measurements should be occuring under the presence of a vibration sequence.
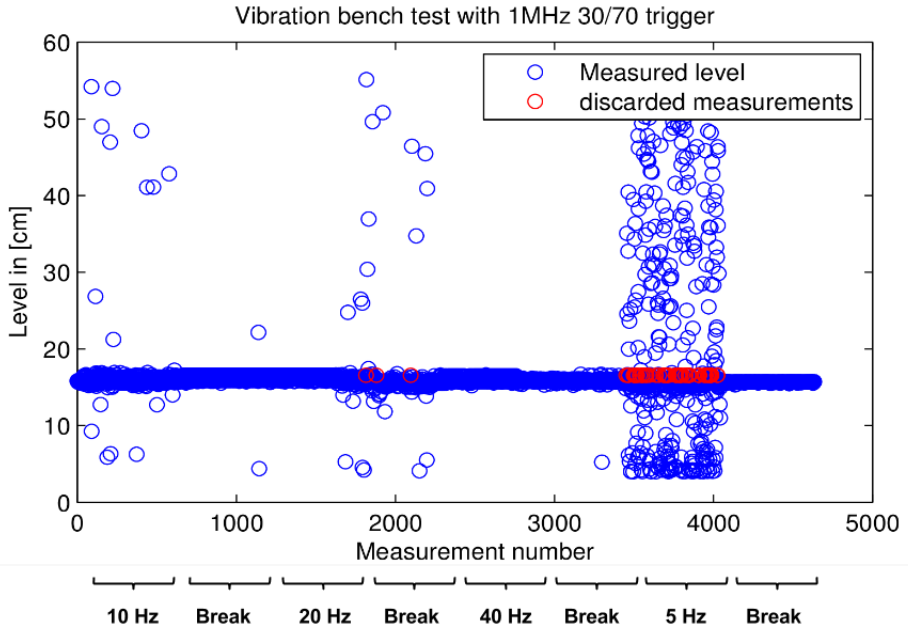
Figure 4.4: Vibration tests guideline

Due to the breaks between each frequency in the vibration program, it is likely that the conditions are more or less ideal before each vibration frequency starts.

4.3.1   Test 1

The initial level in test 1 is given as 16 cm. It is assumed that this is the correct level.

It was discovered after the test was finished that the noise level in this test is quite high. Thus, when the signal strength is low, the high noise will "drown" the echo in the measurement, and it can be difficult to detect the echo. Thus some of the measurements had to be discarded as the echo strength might be of sufficient magnitude, but the high noise levels devours the echo and thus some measurements have to be discarded.

The number of total- and discarded measurements are given in the following table:

	Frequency [MHz]	Total measurements	Discarded measurements
Trigger 1	0.58	4629	317
Trigger 2	1	4630	2447
Trigger 3	1	4633	4192

The results for the three different triggers as described in section 3.10 is given in the following figures. Discarded measurements are marked with red.
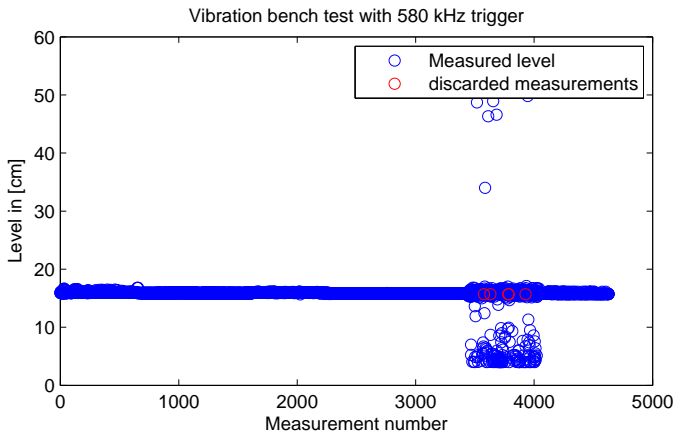
Figure 4.5: Results for 580kHz trigger test 1
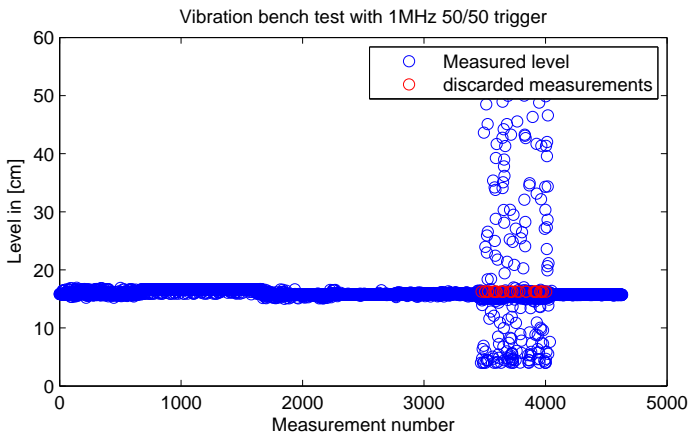
Figure 4.6: Results for 1MHz 50/50 trigger test 1
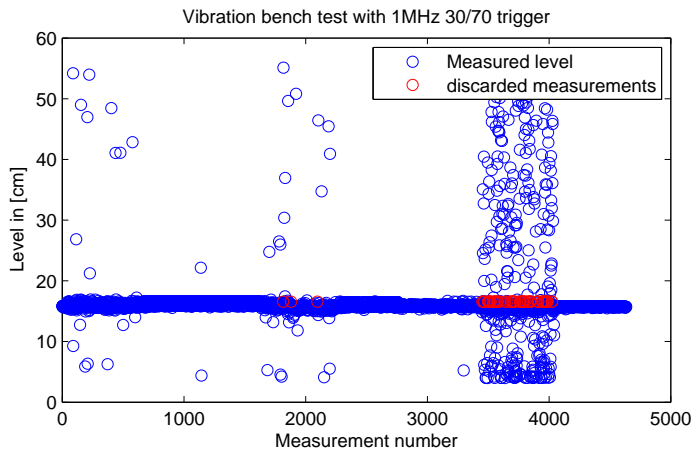
Figure 4.7: Results for 1MHz 50/50 trigger test 1

4.3.2 Test 2

In the second test, the liquid level in the tank was increased. A short test under good conditions was performed as to know what the actual level is inside the tank. The tank level was found to be 31.92 cm.

The number of discarded measurements are presented in table 4.1.

Table 4.1: measurements overview test 2

	Frequency [MHz]	Total measurements	Discarded measurements
Trigger 1	0.58	5630	3
Trigger 2	1	5634	74
Trigger 3	1	5741	141
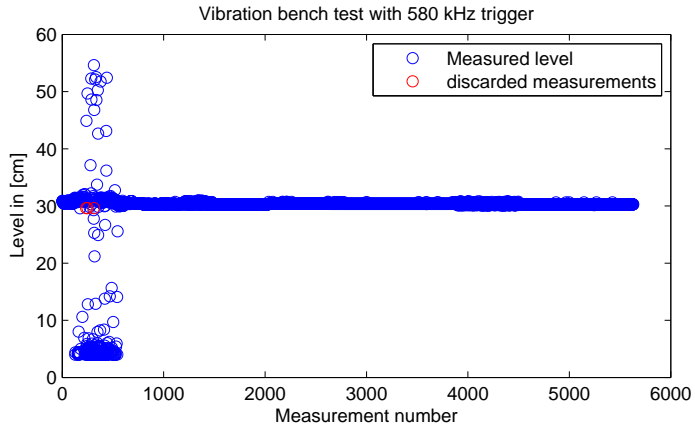
Figure 4.8: Results for 580kHz trigger test 2
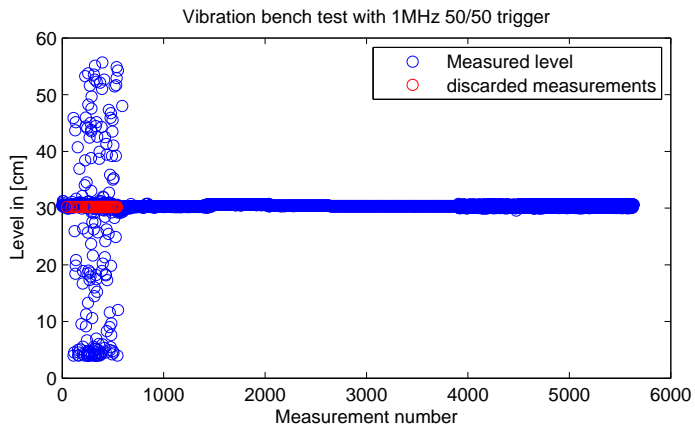
Figure 4.9: Results for 1MHz 50/50 trigger test 2
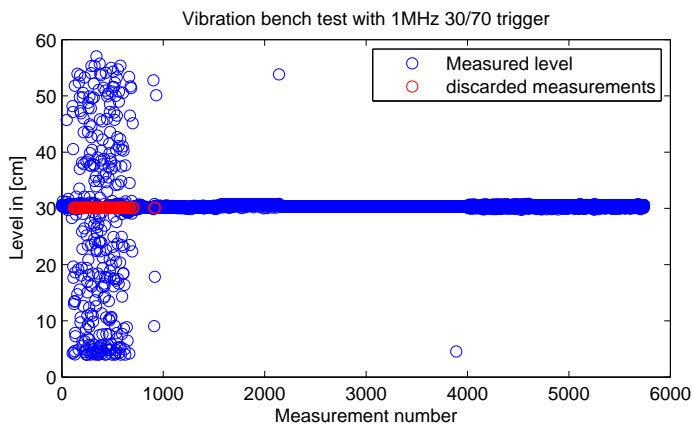
Figure 4.10: Results for 1MHz 50/50 trigger test 2

4.3.3   Test 3

The liquid level was increased again for the third test. The level was found
to be 39.6 cm.

	Frequency $[MHz]$	Total measurements	Discarded measurements
Trigger 1	0.58	5146	0
Trigger 2	1	5142	0
Trigger 3	1	5148	0
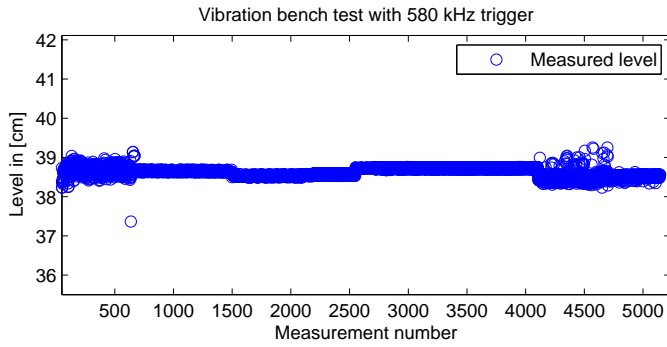
Figure 4.11: Results for 580kHz trigger test 2
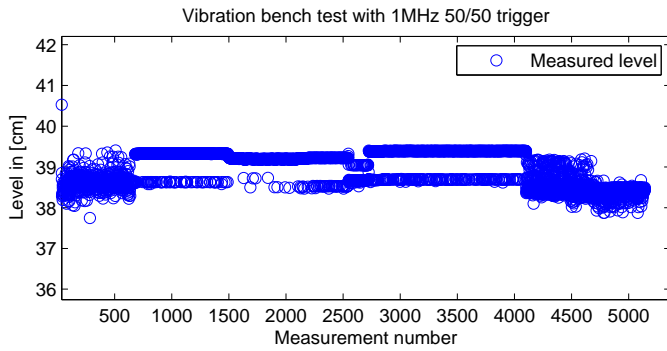
Figure 4.12: Results for 1MHz 50/50 trigger test 2
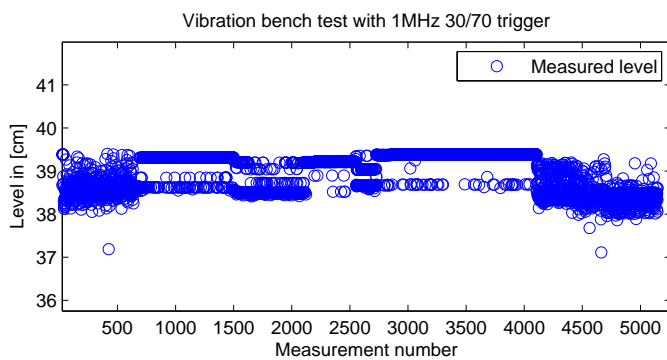
Figure 4.13: Results for 1MHz 50/50 trigger test 2

4.3.4 Vibration test accuracy

The accuracy of the 580 kHz trigger is shown for all three tests, as the 580 kHz had the least number of discarded frequencies. Discarded measurements are not shown.
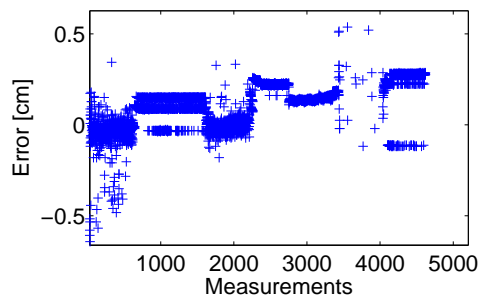
Figure 4.14: Accuracy for the 580 kHz trigger, test 1
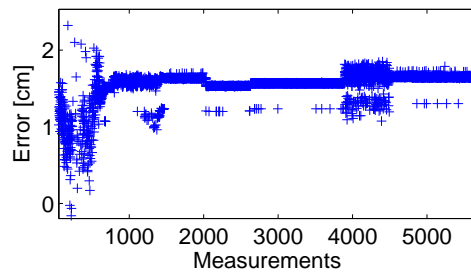
Figure 4.15: Accuracy for the 580 kHz trigger, test 2
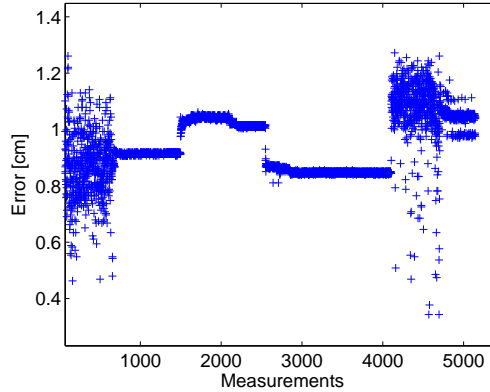
Figure 4.16: Accuracy for the 580 kHz trigger, test 3

As can be seen from figures 4.14-4.16, the accuracy of vibrations test 1 has the least offset while test 2 have over 1 cm in more or less constant error of 1 cm, while test 3 has slightly less than 1 cm.

4.4   Bubbles

To study the effect the frequency of the ultrasonic signal has against bubbles, the following test procedure was created:

1. The transducer is triggered with 4 pulses with a frequency of 1 MHz.

2. Bubbles are added into the tank until the returning echo has completely diminished.

3. The trigger is then changed to 12 pulses with a frequency of 580 kHz.

4. After a 100 triggers as described in 3), the trigger is changed back to 4 1MHz pulses.

The motivation behind this experiment is to see whether changing the frequency of signal will result in more of a returning echo, i.e. if one of the frequencies does not yield any echo, changing to the other frequency might result in a returning signal.

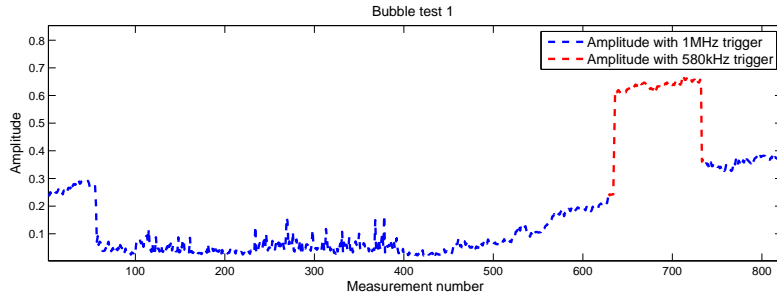Two tests were performed with the test program presented above. They are presented in 4.17 and 4.18.
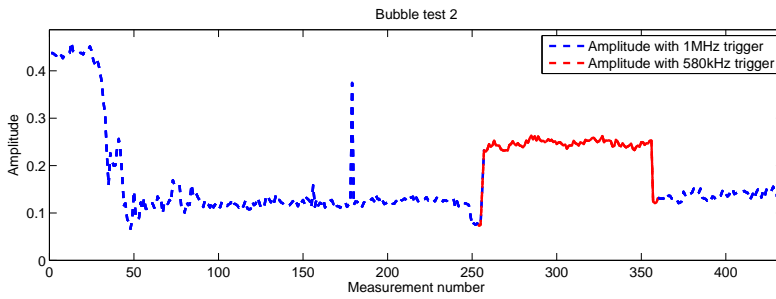
Figure 4.17: Bubble test 1

Figure 4.18: Bubble test 2

It is seen in the figures that the signal level increases when the trigger is changed. An example of the transition can be seen in 4.19.
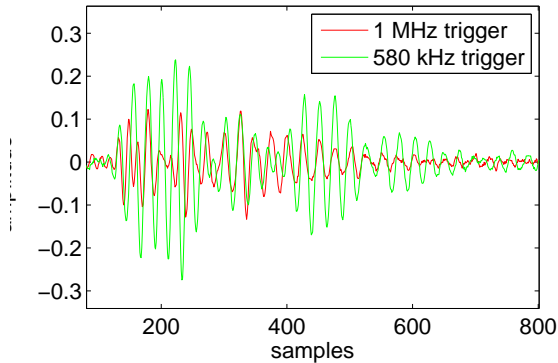

Figure 4.19: Transition from 1 MHz trigger to 580 kHz trigger

4.5 Diesel layer detection

4.5.1 Echo detection with diesel layer

The diesel layer test were performed as described in section 3.11.1. The results are shown in figures 4.20 - 4.23. The echo detection algorithm is able to detect the first echo for all the tests, the main echo, and also at least one echo after the main echo.

As can be seen from figures 4.20-4.23, the echo detection algorithm detect misses some of the echoes that are visible to the human eye. It is still
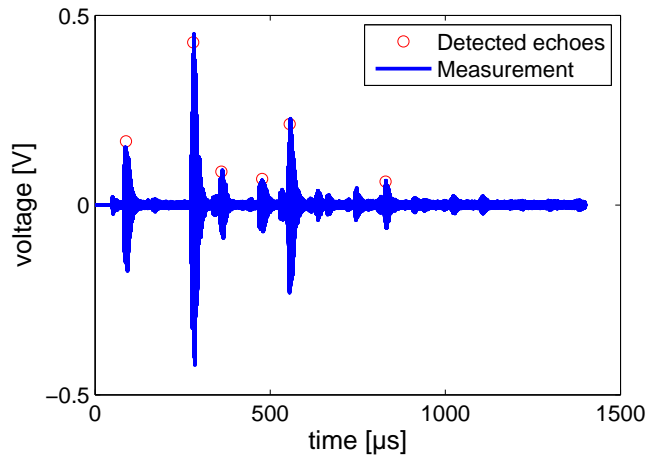
Figure 4.20: Diesel Layer Test 1

able to detect at least two echoes that do not have RTTs that are periodical. A interesting result is that for all tests, the second echo is stronger than the first echo.
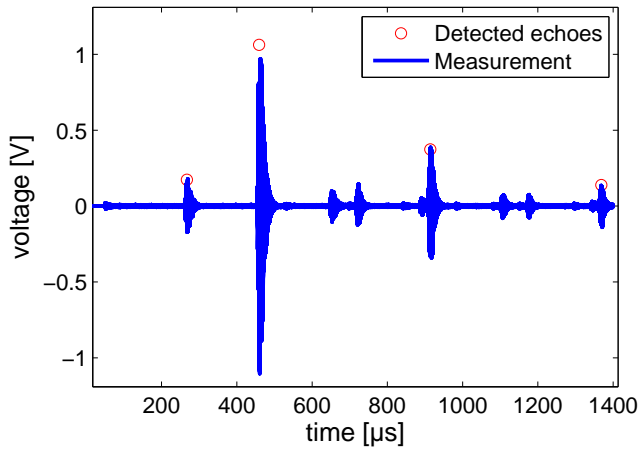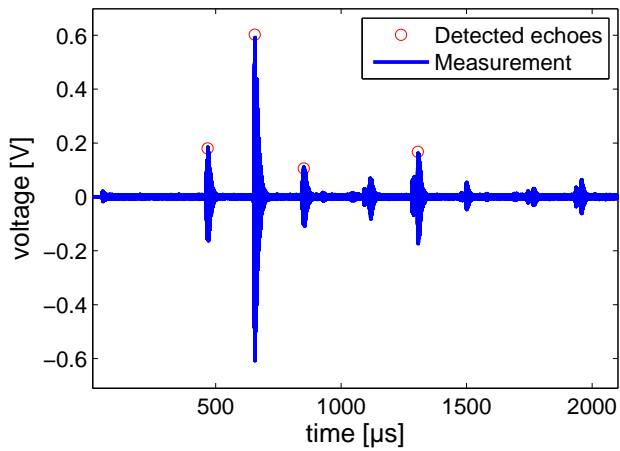
Figure 4.21: Diesel Layer Test 2
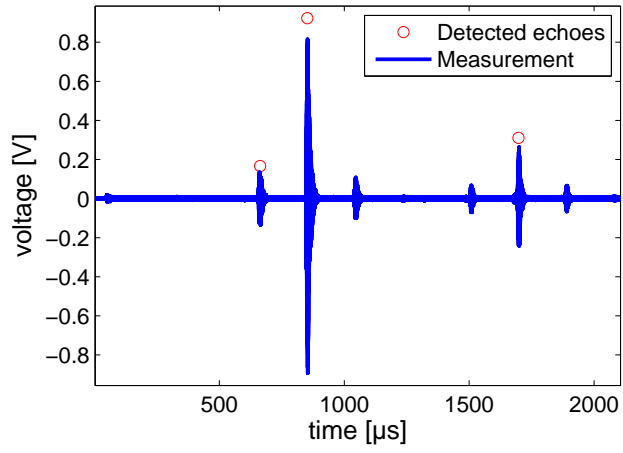

Figure 4.22: Diesel Layer Test 3

Figure 4.23: Diesel Layer Test 4

4.5.2 Frequency analysis

The following figures are the power spectrum density for the first and second echo in the diesel tests which were trigger with 4 1MHz pulses. As is seen in figures 4.24 - 4.27, the frequency content of the first and second echo differ from each other. The first echo contains proportionally more of both of the resonance frequencies, while the second echo has an overweight of 1 MHz for all tests except the first test, in which the 580 kHz frequency is dominating.
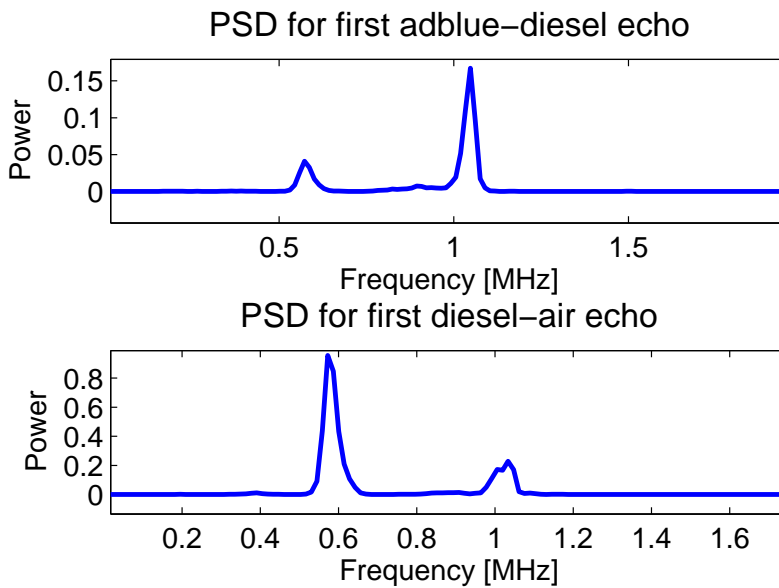

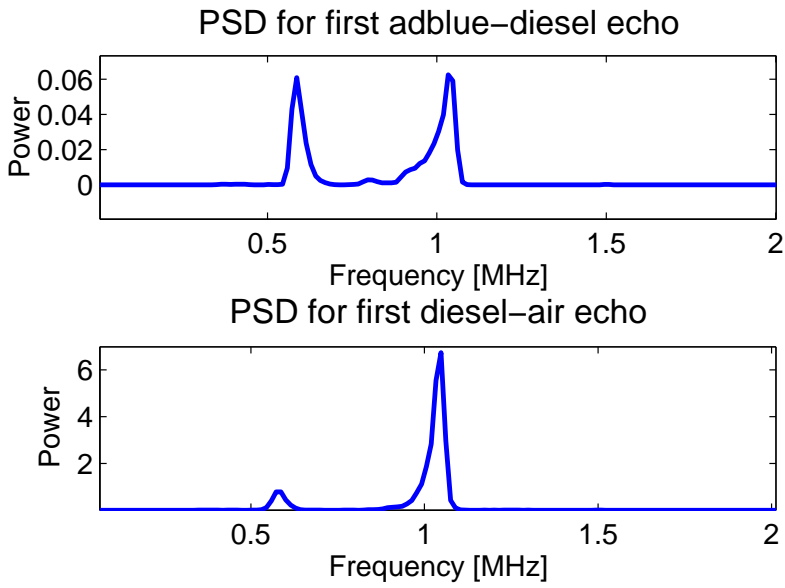Figure 4.24: Diesel Layer Frequency Spectrum Test 1

Figure 4.25: Diesel Layer Frequency Spectrum Test 2

In either case, the frequency content of the first and second echo is seen to be of a different nature for the tests performed in this thesis. It does however seem to be a factor of the thickness of the layers.
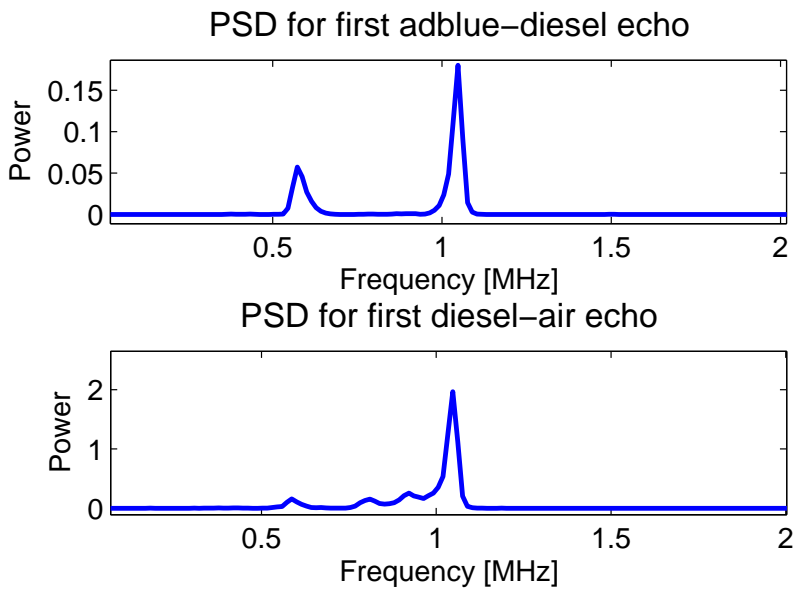
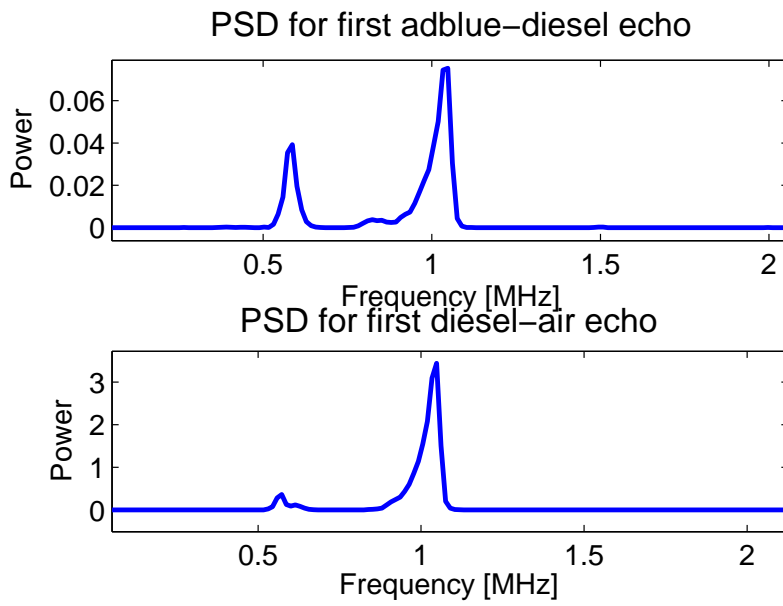Figure 4.26: Diesel Layer Frequency Spectrum Test 3

Figure 4.27: Diesel Layer Frequency Spectrum Test 4

4.6 New filter coefficients

The amplification of the 580 kHz frequency with the new filter coefficients is seen in figures 4.28-4.29. As is seen in figure 4.29, even with a trigger with a 1 MHz frequency, the 580 kHz is of a larger magnitude than the 1 MHz frequency. The power spectrum density for the 1 MHz trigger is seen in figure 4.30.

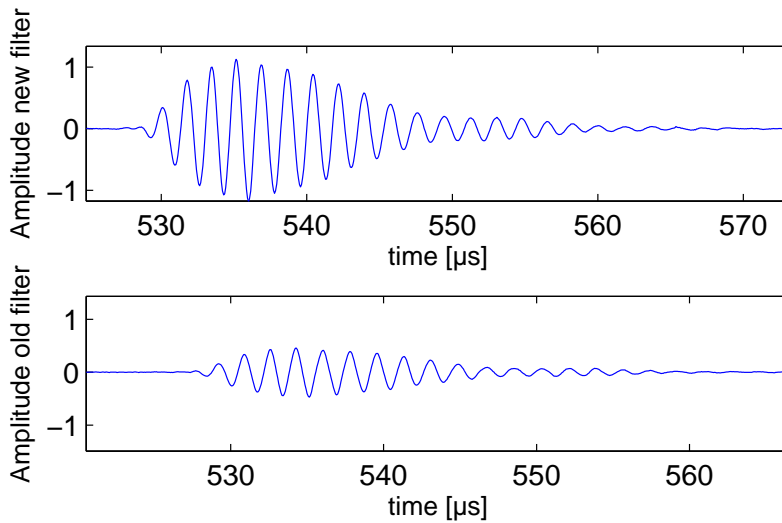### 4.6.1 580 kHz trigger

Figure 4.28: New versus old filter amplitude with 580 kHz trigger
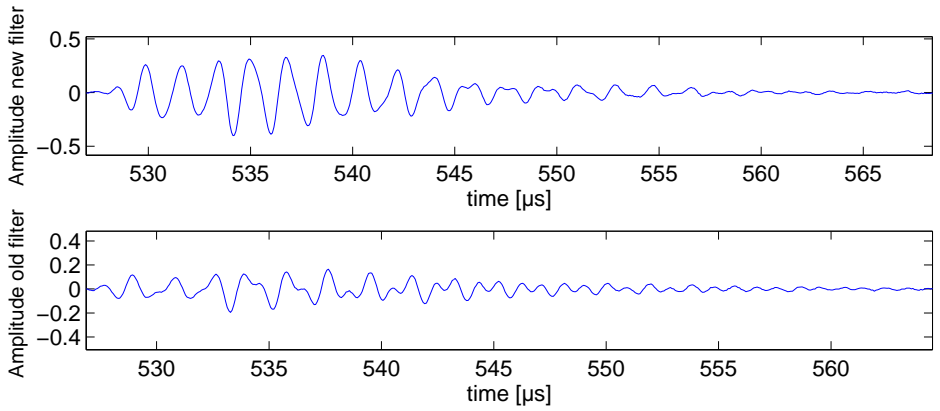
4.6.2   1MHz trigger

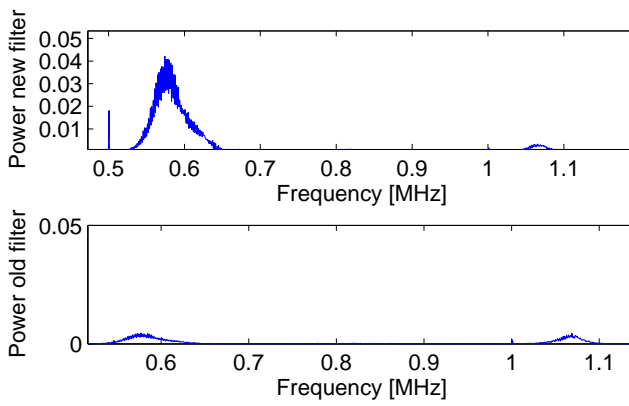Figure 4.29: New versus old filter amplitude with 1MHz trigger

Figure 4.30: New versus old filter PSD plot with 1MHz trigger

Chapter 5

Discussion

5.1 The amplitude of the echo

The amplitude of the returning echo is vital as to be able to measure the liquid level. The experimental results presented in section 4.1 show that the amplitude of the returning echo is a factor of the ultrasonic signal frequency, the number of pulses in the trigger, and the liquid level. Thus, the choice of trigger has a significant impact on the performance of the system, in regard to how many pulses are used in the trigger. This can be seen from the experimental data, as for both frequencies the 4 pulse trigger have the overall highest amplitude. The simulation model presented in section 3.4 have results which shows the same trend as the experimental data in terms of echo amplitude, and with further improvements might be used to further explore which trigger is best suited. The simulation model has its drawbacks, as it is only in 2D, does not account for directivity, and the ultrasonic echo received in the simulations does not resemble the actual received echo in structure. It is not known if it possible to implement the model in 3D, but

this would allow for directivity and also be more like the actual system. For the purposes of studying the received echo amplitude the 2D model might be enough, but this should be explored by fit the model as closely to reality as possible.

5.2 Triggers

Regarding frequency, the resonance frequency of 580 kHz performs better in terms of signal strength, and is thus found to be more noise resistant than the frequency of 1 MHz. This can be seen in both the vibration tests and the bubbles tests. The 580 kHz frequency yields fewer discarded measurements than both triggers at 1 MHz, under the same conditions. It is also shown to have better performance versus bubbles under conditions in which the signal at 1 MHz give little or no returning echo. Changing the response of the bandpass filter to amplify the 580 kHz resonance frequency with the same magnitude as the 1 MHz frequency will give more signal strength. It is also interesting to note that the echo resulting from the trigger at 1MHz has larger amplitude with the new bandpass filter.

5.3 Accuracy

Due to the time-frame of the project, the echo start finder was not repeatedly tested to find the parameters in algorithm 3 which were most suited for each trigger. The performance of the echo start finder is therefore not to be considered optimal. Also, due to the distance in time between each trigger of the same type being 1.5 seconds, the measurements are deemed to have too large a break between them as for averaging to have the desired effect. As the measurements in the vibration tests contain a relatively high

noise level, the algorithm will often jump with a period of the frequency present in the measurements. In order to test how accurate the echo start finder can get, the parameters need to be optimized as to get as accurate results under different liquid levels and conditions as possible.

The large deviations seen in the vibration tests 2 and 3 are not the fault of the echo finder, as is discovered by manual inspection. Under the 5 Hz and 10 Hz vibration, the echo shifts position in consecutive measurements. This might be due to the fact that the 5 and 10 Hz vibration frequency has the largest amplitude in vibration, that is, moving the tank more than the other frequencies. This might also be the reason for the constant error, due to the fact that the actual level is calculated based on measurements taken before the vibration tests are started. The pipe in the prototype is fastened with duct tape, and could therefore actually move when the vibration starts. Therefore, the echo might actually not be phase shifted due to the impact the vibration has on the ultrasonic signal, but as a cause of the prototype pipe moving slightly. As the vibration program starts with the 5 Hz frequency, which has the biggest amplitude in terms of moving the prototype sideways, this might dislocate the pipe compared to the tests taken before the vibration starts.

5.4 Echo-detection and start-finder algorithm

The algorithms presented in 2 and 3 are highly dependent on the parameters involved. The values for these parameters used in this thesis are not based on large amounts of data, more on a heuristic approach as to test the algorithms. Also, the algorithms can be suited to a specific trigger in a more direct way, by for instance relying more heavily on the 580 kHz correlation for the 580 kHz trigger, and vice versa for the 1 MHz trigger.

This might further improve the echo detection algorithm. This also applies for the start-finder algorithm.

5.5   Diesel detection

Analysis from the diesel data show that for the given tests that were executed, it is possible to detect multiple echoes with the echo detector. How many echoes that will be detected is highly dependent on the settings in the echo detector presented in algorithm 2, and also on the thickness of the layers. Indications of diesel and adblue present in the tank is still detectable, namely by combining the following properties:

1. If the second echo is stronger than the first echo. This situation has never been observed for tests with only adblue.

2. Multiple echoes are present, and RTTs of said echoes are not multiples of each other.

3. The frequency content of the first and second echo. Even though the four tests with PSD analysis in section 4.5.2 have different PSDs, the first echoes frequency content differ from that of the second echo.

All of the above depend on the echo detection, and this is thus a very vital part in finding the presence of an extra liquid layer. If only the first and the last properties are necessary for the diesel to be detected, the echo detected does not have to detect the third echo. This simplifies the detection of the extra layer, but it is not whether this will be enough for detecting diesel layers in a robust way. The second property is also dependent on the echo start finder algorithm, and thus is the most difficult property to detect.

Chapter 6

Future work

The next phase in development would first and foremost be to decide on which combination of triggers that should be used. Also the trigging time should be reduced to an absolute minimum (which depends on the maximum level in the tank). Thus, averaging consecutive measurements might be so close to each other in time that this will reduce random noise. A new prototype should be developed, with the aim to be more sturdy than the current prototype. The simulator could improved to resemble the system more, and thus the most efficient settings for the pipe could be investigated and tested, in terms of pipe radius and material. The new data could then be used to tune the algorithms presented in this thesis. After making the next prototype, new data could be created. The algorithms could then be tailored to the trigger that is used in the new prototype. Thereafter, the combination of temperature changes and vibrations should be tested alongside to investigate the overall robustness and accuracy of the system. Lastly, it should be explored how thick of a diesel layer that can be poured into the tank before the system detects it, and if this is sufficient.

Bibliography

[1] European Enviromental Agency. Nitrogen oxides (nox) emissions (ape 002). Technical report, European union, 2014.

[2] M. Karthikeyan S. Prabhakar and V. N. Banugopan. Control of emission characteristics by using selective catalytic reduction (scr) in d.i. diesel engine. *IEEE*, 2010.

[3] E. B. Steinberg. Ultrasonics in industry. *IEEE*, 1965.

[4] L. R. Rod. Ultrasonic liquid level sensor. *IEEE*, 1956.

[5] Håkon Bøe. Level measurement. Technical report, NTNU, 2013.

[6] Bernt Inge Hansen and Jarle André Johansen. Experimental results on the pressure dependence of the minnaert resonance frequency for nitrogen gas bubbles in water. *IEEE*, 2011.

[7] Ni labview interface for arduino toolkit. `http://sine.ni.com/nips/cds/view/p/lang/no/nid/209835`.

[8] Arduino port manipulation due. `http://www.arduino.cc/en/Reference/PortManipulation`.

[9] DAF Trucks Limited. Adblue: The facts a handbook for adblue users. `http://www.daf.eu/SiteCollectionDocuments/UK/adblue_the_facts.pdf`, June 2009.

[10] Comsol multiphysics. `http://www.comsol.com/`.

[11] Kui Sun Hanxin Chen. Simulation of ultrasonic testing technique by finite element method. *IEEE*, 2012.

[12] T. Douglas Mast et al. A k-space method for large-scale models of wave propagation in tissue. *IEEE*, 2001.

[13] k-wave a matlab toolbox for the time-domain simulation of acoustic wave fields. `http://www.k-wave.org/`, 2011.

[14] k-wave manual. `http://www.k-wave.org/manual/k-wave_user_manual_1.0.1.pdf`, 2011.

[15] Shenitech. `http://www.shenitech.com/support/support_soundspeed.htm`.

[16] J. M. M. Pinkerton. The absorption of ultrasonic waves in liquids and its relation to molecular constitution. *Proceedings of the Physical Society*, 1949.

[17] L.W. Nagel and D.O. Pederson. Spice (simulation program with integrated circuit emphasis. Technical report, University of Berkeley, College of Engineering, 1973.

[18] Linear technology ltspice. `http://www.linear.com/designtools/software/#LTspice`.